INSTITUTO POLITÉCNICO NACIONAL

Centro Interdisciplinario de Investigación para el Desarrollo Integral Regional Unidad Oaxaca

Doctorado en ciencias en conservación

y aprovechamiento de recursos naturales

(Patrones y procesos para la biodiversidad del neotrópico)

Estudio de señales ultrasónicas de materiales basados en cemento durante procesos de hidratación, carbonatación y penetración de cloruros

Tesis que para obtener el grado académico de:

Doctor en ciencias

Presenta:

M. en C. Mario Fernando Cosmes López

Directores de tesis:

Dr. Francisco Castellanos León

Dr. Prisciliano Felipe de Jesús Cano Barrita

Índice

SIP-14 bis

INSTITUTO POLITECNICO NACIONAL

SECRETARIA DE INVESTIGACION Y POSGRADO

ACTA DE REVISION DE TESIS

En la Ciudad de Oaxaca de Juárez siendo las 13:00 horas del día 29 del mes de noviembre del 2016 se reunieron los miembros de la Comisión Revisora de Tesis designada por el Colegio de Profesores de Estudios de Posgrado e Investigación del **Centro Interdisciplinario de Investigación para el Desarrollo Integral Regional, Unidad Oaxaca (CIIDIR-OAXACA)** para examinar la tesis de grado titulada: **"Estudio de señales ultrasónicas de materiales basados en cemento durante procesos de hidratación, carbonatación y penetración de cloruros**

Presentada por el alumno

Cosmes	**López**	**Mario Fernando**
Apellido paterno	materno	nombre(s)

Con registro: | B | 1 | 2 | 0 | 1 | 5 | 1 |

aspirante al grado de: **DOCTORADO EN CIENCIAS EN CONSERVACIÓN Y APROVECHAMIENTO DE RECURSOS NATURALES**

Después de intercambiar opiniones los miembros de la Comisión manifestaron ***SU APROBACION DE LA TESIS***, en virtud de que satisface los requisitos señalados por las disposiciones reglamentarias vigentes.

LA COMISIÓN REVISORA

Directores de tesis

Dr. Francisco Castellanos León

Dr. Prisciliano Felipe de Jesús Cano Barrita

Dr. Sadoth Sandoval Torres

Dra. Lucita Lagunez Rivera

Dra. Lucia Medina Gómez

PRESIDENTE DEL COLEGIO DE PROFESORES

Dr. Salvador Isidro Belmonte Jiménez

CENTRO INTERDISCIPLINARIO DE INVESTIGACION PARA EL DESARROLLO INTEGRAL REGIONAL C.I.I.D.I.R. UNIDAD OAXACA I.P.N.

INSTITUTO POLITÉCNICO NACIONAL

SECRETARÍA DE INVESTIGACIÓN Y POSGRADO

CARTA CESION DE DERECHOS

En la Ciudad de Oaxaca de Juárez el día 02 del mes diciembre del año 2016, el (la) que suscribe **Cosmes López Mario Fernando** alumno (a) del Programa de **DOCTORADO EN CIENCIAS EN CONSERVACIÓN Y APROVECHAMIENTO DE RECURSOS NATURALES** con número de registro B120151, adscrito al Centro Interdisciplinario de Investigación para el Desarrollo Integral Regional, Unidad Oaxaca, manifiesta que es autor (a) intelectual del presente trabajo de Tesis bajo la dirección de los Dres. Francisco Castellanos León y Prisciliano Felipe de Jesús Cano Barrita y cede los derechos del trabajo titulado: **"Estudio de señales ultrasónicas de materiales basados en cemento durante procesos de hidratación, carbonatación y penetración de cloruros"** Al Instituto Politécnico Nacional para su difusión, con fines académicos y de investigación.

Los usuarios de la información no deben reproducir el contenido textual, gráficas o datos del trabajo sin el permiso expreso del autor y/o director del trabajo. Este puede ser obtenido escribiendo a la siguiente dirección **Calle Hornos 1003, Santa Cruz Xoxocotlán, Oaxaca**, e-mail: posgradoax@ipn.mx ó mariofernandocl@gmail.com Si el permiso se otorga, el usuario deberá dar el agradecimiento correspondiente y citar la fuente del mismo.

Cosmes López Mario Fernando

CENTRO INTERDISCIPLINARIO
DE INVESTIGACION PARA EL
DESARROLLO INTEGRAL REGIONAL
C.I.I.D.I.R.
UNIDAD OAXACA
I.P.N.

Introducción general

El concrete es una pieza clave en la industria de la construcción en todo el mundo, como carreteras, presas, puentes, edificios, entre otros. Dichas estructuras están continuamente sujetas a efectos que degradan su integridad estructural provocando un riesgo de seguridad, por lo tanto, se deben desarrollar alternativas para una evaluación efectiva de su calidad sin la necesidad de dañar las estructuras estudiadas [1].

En este sentido, el uso de pruebas no destructivas constituye una interesante estrategia para el monitoreo y evaluación del estado de las estructuras de concreto sin dañar su apariencia o rendimiento [2]. Las pruebas no destructivas con ultrasonido se basan en la propagación de ondas a través del elemento analizado y han sido ampliamente aplicadas en estructuras de concreto [3,4]. La velocidad de propagación de las ondas ultrasónicas depende de distintas características del material como: densidad, módulo de elasticidad (E) y coeficiente de Poisson, (μ); sus principales aplicaciones son la detección de daños y evaluación de condiciones iniciales del concreto [5].

En general la aplicación de los análisis no destructivos por ultrasonido se ha hecho usando dos métodos convencionales, la transmisión directa y el pulso eco [6]. En el método de transmisión se realiza la medición en lados opuestos de la estructura, para conocer el tiempo de recorrido que junto con la distancia recorrida nos permite conocer la Velocidad de Pulso Ultrasónico (UPV). El pulso eco, mide la reflexión por medio del mismo u otros transductores que actúan como receptores del pulso ultrasónico. Las pruebas anteriores se han estandarizado por medio de

procedimientos, instrumentaciones y análisis de datos para distintos tipos de ondas aplicadas a estructuras de concreto [7].

Cualquier variación en la velocidad de propagación de las ondas ultrasónicas indican vacíos, no uniformidad del material o daños [8,9]. Como señalan varios autores [10,11,12], las ondas ultrasónicas pueden verse afectados por varios factores, como la condición superficial, la humedad, la presencia de refuerzos y principalmente la composición del concreto. Tales factores provocan variaciones no solo en la velocidad de propagación de las ondas ultrasónicas, sino también en la señal en el tiempo, lo que dificulta el análisis de resultados [13]. Sin embargo, este hecho abre una ventana de oportunidad para poder conocer otras propiedades además del VPU, que permitan la evaluación de distintos fenómenos de una manera completamente no destructiva.

Debido a que la mayor cantidad de reacciones que suceden dentro del concreto se llevan a cabo en la pasta de cemento, el siguiente trabajo se centra en el análisis del comportamiento de la pasta de cemento en distintas condiciones, por medio de ondas longitudinales y transversales, con un intervalo de frecuencia de 50 kHz a 2250 kHz. Este trabajo se encuentra dividido en tres partes:

La primera parte, presenta el estudio de especiemos de concreto con el objetivo de identificar frecuencias especificas relacionadas con agregados y pasta de cemento durante la hidratación del concreto, por medio del análisis de transformada de Fourier de la respuesta ultrasónica de especímenes de concreto con diferentes frecuencias de excitación. Con lo que fue posible identificar el comportamiento de la pasta de cemento y agregados en el dominio de la frecuencia.

En la segunda parte, se estudió la respuesta ultrasónica en pastas de cemento con tres relaciones agua cemento (a/c = 0.60, 0.50 y 0.40). Los especímenes fueron expuestos a la carbonatación acelerada en una cámara ambiental a 30℃, 65% de humedad relativa, y 4% CO2 (v / v). Los resultados muestran que es posible evaluar el grado de carbonatación de los especímenes de pasta de cemento por medio del análisis en el dominio de frecuencia en función del tiempo de exposición, de los cambios relacionados a la carbonatación, independientemente de la relación agua / cemento.

La tercera parte presenta, presenta el estudio de dieciocho especímenes de pasta de cemento con una relación a / c = 0.55, con 100% de cemento Portland ordinario, sustitución del 20% y 40% de cemento por cenizas volantes de clase F y sustitución al 10% por humo de sílice. Los especímenes fueron secados en horno y saturados a 4,08 bar con soluciones de NaCl de 16,5% (2,8 M), 33% (5,6 M) y una con agua desionizada, como control. Los resultados muestran que, aplicando la metodología utilizada en las secciones anteriores y tomando como base los resultados del control, es posible distinguir entre las dos concentraciones de NaCl independientemente de las adiciones minerales y entre las pastas de cemento con adiciones minerales dependiendo de su capacidad de ligado.

Referencias

[1]. Mehta, P. K. (1986). Concrete. Structure, properties and materials.

[2]. Hoła, J., & Schabowicz, K. (2010). State-of-the-art non-destructive methods for diagnostic testing of building structures–anticipated development trends. Archives of Civil and Mechanical Engineering, 10(3), 5-18.

[3]. Philippidis, T. P., & Aggelis, D. G. (2003). An acousto-ultrasonic approach for the determination of water-to-cement ratio in concrete. Cement and Concrete Research, 33(4), 525-538.

[4]. Lai, W. L., Wang, Y. H., Kou, S. C., & Poon, C. S. (2013). Dispersion of ultrasonic guided surface wave by honeycomb in early-aged concrete. NDT & E International, 57, 7-16.

[5]. Panesar, D. K., & Chidiac, S. E. (2007). Ultrasonic pulse velocity for determining the early age properties of dry-cast concrete containing ground granulated blast-furnace slag. Canadian Journal of Civil Engineering, 34(5), 682-685.

[6]. Malhotra, V. M., & Carino, N. J. (2003). Handbook on Nondestructive Testing of Concrete Second Edition. CRC press.

[7]. Davis, A. G., Ansari, F., Gaynor, R. D., Lozen, K. M., Rowe, T. J., Caratin, H., ... & Hertlein, B. H. (1998). Nondestructive test methods for evaluation of concrete in structures. American Concrete Institute, ACI, 228.

[8]. Whitehurst, E. A. (1986). Evaluation of concrete properties from sonic tests. ACI Monograph, 2, 73.

[9]. Carino, N. J. (1997). Nondestructive test methods. Concrete construction engineering handbook, 1.

[10]. Popovics, J. S. (2003). NDE techniques for concrete and masonry structures. Progress in Structural Engineering and Materials, 5(2), 49-59.

[11]. Schabowicz, K. (2014). Ultrasonic tomography–the latest nondestructive technique for testing concrete members–description, test methodology, application example. archives of civil and mechanical engineering, 14(2), 295-303.

[12]. Schabowicz, K., & Suvorov, V. (2014). Non-destructive testing and constructing profiles of back walls by means of ultrasonic tomography. Russian J. Non-destructive Testing, 50(2), 109-119.

[13]. Abo-Qudais, S. A. (2005). Effect of concrete mixing parameters on propagation of ultrasonic waves. Construction and building materials, 19(4), 257-263.

Capítulo I

Ultrasound frequency analysis for identification of aggregates and cement paste in concrete

Mario F. Cosmes-López[1], Francisco Castellanos[2*], Prisciliano F. de J. Cano-Barrita[2]

[1] *PhD student at Instituto Politecnico Nacional, CIIDIR Unidad Oaxaca, Hornos No. 1003, Santa Cruz Xoxocotlán, Oaxaca, Mexico, C.P. 71230.*

[2] *Researcher at Instituto Politecnico Nacional, CIIDIR Unidad Oaxaca, Hornos No. 1003, Santa Cruz Xoxocotlán, Oaxaca, Mexico, C.P. 71230.*

Phone: + 52 951 5170610, Emails: mcosmesl1200@alumno.ipn.mx, fcastellanos@ipn.mx and pcano@ipn.mx

*Corresponding author

Abstract

The aim of the present study was to identify specific frequencies related to aggregates and cement paste during concrete hydration, by performing a Fourier analysis of the ultrasonic response of concrete specimens to different excitation frequencies. This identification will reduce the high influence of aggregates in the ultrasound signal analysis, enabling a better assessment of changes occurring in the cement paste. Thirty-five cylindrical specimens with a diameter of 100 mm and a length of 200 mm were cast with a water to cement ratio = 0.60. Thirty specimens were destructively tested at 1, 3, 5, 7, 14 and 28 days for their compressive strength. The remaining five specimens were non-destructively tested at 1, 3, 5, 7, 14, 28 and 56 days using longitudinal and transversal ultrasonic wave transducers with frequencies from 50 kHz to 500 kHz. Analysis of the evolution in frequency observed in the specimens identified variations related to progressive hydration of the cement paste, in contrast with the invariant behavior of the inert aggregates. Results show that it is possible to distinguish the behavior of cement paste and aggregates in the frequency domain. As a consequence, it should be possible in future research to evaluate more efficiently different phenomena that affect only the cement paste.

Keywords

Ultrasound; Fourier analysis; frequency bands; cement paste; aggregates; hydration

1. Introduction

Non-destructive techniques are used to evaluate the quality and performance of concrete structures without causing any structural damage [1, 2]. The Ultrasonic Pulse Velocity (UPV) is one of the most used non-destructive techniques for measuring mechanical properties of concrete during hydration and evaluating damage in concrete structures [3-6]. Previous studies have found an exponential relationship between the compressive strength of concrete and the UPV, which has shown to be barely sensitive to small variations in strength at late ages [7-8]. Concrete is basically composed of a mixture of cement, water, fine and coarse aggregates that produce a heterogeneous material. The heterogeneities produced by the coarse aggregates strongly influence the propagation of ultrasonic waves, depending on the frequency studied [9]. Therefore, the analysis of changes in an ultrasound wave propagated across a concrete specimen at selected frequencies, may be used to extract information on processes occurring mainly in the cement paste, for example during hydration or during chemical reactions in the cement paste with aggressive species (e.g. chlorides and CO_2).

When a wave propagates, its phase and amplitude are modified depending on the transmission medium. The propagation of ultrasound waves is affected by the heterogeneities of concrete in different ways. The influence depends on the wavelength and the size of the concrete components [10]. In previous studies, this behavior was used to characterize entrained air voids in cement paste [11]. Other studies have employed the propagation velocity of the wave attenuation to estimate cracking [12-14], voids, the setting process [15, 16] and the compressive strength of concrete. Taking advantage of these properties, several experimental studies using through-transmission ultrasonic measurements of longitudinal or transversal waves have been carried out on

concrete to determine the setting time of concrete [4,17]. It has also been found that the attenuation of the ultrasound signal is different for cement paste, mortar and concrete in a frequency range of 50 - 1000 kHz [18-19]. Additionally, the setting process of cement pastes has been analyzed by the response of ultrasonic waves using the frequency spectrum of the Fast Fourier Transform [20].

Based on the aforementioned, it is assumed that, depending on the frequency band used, the response of concrete materials to ultrasonic waves contains more information than is reported. Therefore, this study focuses on developing a method for the identification of frequency bands associated with aggregate and cement paste during the hydration process of concrete. This identification would enhance the study of process which occur only in the cement paste such as hydration, chloride penetration and binding as well as carbonation produced by the chemical reaction between the CO_2 and $Ca(OH)_2$ dissolved in the pore fluid.

2. Experimental procedure

2.1. Materials

Mexican ordinary Portland cement class 30RS (ASTM C150 Type I or EN 197-I, with chemical composition shown in Table 1) was used. The coarse aggregate was limestone with a maximum size of 13 mm. The fine aggregate was river sand with a fineness module of 2.67. Thirty-five cylindrical specimens measuring 100 mm in diameter and 200 mm in height were cast with a w/c ratio of 0.60. After 1 day, the specimens were stripped and moist-cured in a saturated lime solution at 23 ± 2 °C for 56 days, according to the standard ASTM C31 [21]. Moist curing with saturated lime solution avoids

leaching of the calcium hydroxide from the cement paste, which otherwise would increase the porosity and reduce the density and elastic modulus of the cement paste.

2.2. Methods

2.2.1. Compressive strength

Thirty specimens were tested at 1, 3, 5, 7, 14, and 28 days to measure their compressive strength using a 120 ton compression machine.

2.2.2. Ultrasonic measurements

Five specimens were tested at 1, 3, 5, 7, 14, 28 and 56 days. The ends of the specimens were cut with a concrete saw in order to obtain a smooth surface. A record was maintained of their responses in through-transmission to longitudinal and transversal ultrasonic waves, generated by eight pairs of transducers with frequencies ranging from 50 kHz to 500 kHz. The position of the transducers and their applied pressure were kept constant during the experiment. Petroleum jelly was used as coupling agent to improve wave transmission. The excitation signal was generated by a 5058PR pulser/receiver with a voltage of 200 V and damping of 40 dB. The UPV was also obtained for the thirty specimens before compressive strength testing.

3. Wave analysis

3.1. Signal processing

The aim of the proposed method for analyzing the ultrasound signals is to identify frequency bands over time associated with aggregates and cement paste in hydraulic concrete. One of the features of concrete is that the properties of the hydrating cement

paste vary over time as opposed to those of aggregates which are invariant over time. The Fast Fourier Transform (FFT) has been recognized as a standard signal processing technique for analyzing ultrasound signals [22]. The first step in the proposed analysis is to calculate the time-discrete Fourier Transform (TDFT) of the ultrasound signal $f(n\Delta t)$, according to Eq. (1).

$$\mathrm{F}(\mathrm{k}\Delta\omega) = \frac{1}{2\pi}\sum_n f(n\Delta t)e^{-i\left(2\pi kn/N\right)}\Delta t \tag{1}$$

where T is the duration of the ultrasound signal, discretized at a sampling rate $\Delta t = T/N$, and $k\Delta w$ are the resulting discrete frequencies.

A window of $\mathrm{F}(\mathrm{k}\Delta\omega)$ is subsequently selected from the frequency response function of the transducers with an intensity greater or equal to 6 dB, as specified by the ultrasound transducer manufacturer.

$$\mathrm{G}(\mathrm{k}\Delta\omega) = \begin{cases} F(k\Delta\omega), & k_1 \leq k \leq k_2 \\ 0, & elsewhere \end{cases} \tag{2}$$

The evolution in time of the seven spectra obtained (1, 3, 5, 7, 14, 28 and 56 days) from ultrasound measurements$\mathrm{G_i}(k\Delta\omega)$ $\mathrm{G_i}(k\Delta\omega)$, where $1 \leq i \leq 7$, was analyzed for the identification of frequency bands associated with aggregates or cement pastes. This analysis consists of the correlation of variations along time of every frequency amplitude $|\mathrm{G_i}(\mathrm{k}\Delta\omega)|$, with a function that describes an assumed behavior of aggregates or cement pastes. For the identification of frequencies k_a associated with aggregates, a correlation with a constant function different from zero was performed. In the case of frequencies k_p related to cement pastes, they were correlated with the evolution in time of the compressive strength that indicates the progress of cement hydration, Fig. 1. The

compressive strength was determined according to the standard ASTM C39 / C39M – 16 [23]. The load was applied at a rate of 0.25 ± 0.05 MPa/s (35 ± 7 psi/s).

Evolution of the compressive strength of concrete is closely related to density (ρ) changes in the hydrating cement paste, influencing the propagation of the ultrasonic waves [2]. Constant density of limestone aggregate (ρ = 2.60 kg/m^3), of sand (ρ = 2.57 kg/m^3) and of saturated concrete were obtained, Fig. 1. A strong correlation coefficient (R=0.98) states the evident similarity between density and compressive strength evolution in time. Similarly, a strong correlation (R=0.984) was found between the compressive strength of concrete (f'c) and UPV.

Once the assumed behavior for cement paste was identified, a threshold was defined as the mean value of the correlations obtained, with a precision of 0.001, for the identification of cement paste or aggregates, assuming a normal distribution for those values. The frequencies with correlations stronger than the threshold were assumed to be related to the corresponding behavior of cement paste or aggregates. As the thresholds for both identifications were independently established, there were atypical frequencies identified with both behaviors that were excluded from the analysis. Finally, the correlations between the energy (E_i) and the functions that describe the assumed behavior were calculated

$$E_i = \sum_{\forall j} \left| G_i\left(k_j \Delta\omega\right) \right|^2 \quad (3)$$

where j denotes the frequencies associated with paste or aggregates, respectively. The time evolution of the calculated energy must be consistent with the corresponding assumed behavior. The wave attenuation and wavelength analysis are two alternative

validations of the proposed method for identifying cement paste and aggregates, presented in the following sections.

3.2. Wave attenuation analysis

The different components in concrete induce a high attenuation mainly correlated with the size of aggregates. This attenuation α is defined as [24]

$$\alpha = -\frac{20}{x} log\left(\frac{A_x}{A_0}\right) \tag{4}$$

where A_0 is the initial amplitude of the wave and A_x is the amplitude after the wave has traveled across the length x.

By using Eq. (4), different attenuation responses were related to cement paste, mortar and concrete [19]. These different behaviors can be utilized to distinguish between concrete and cement paste depending on the frequency used. The attenuation can be correlated with the scattering of ultrasonic waves through the material, and in the case of concrete, this scattering has been linked to the presence of aggregates [19]. Philippidis and Aggelis [19] found that the attenuation in cement paste specimens is higher in low frequencies than in high frequencies relative to the attenuation obtained in concrete specimens. Other studies support these findings [18, 25]. If the identified frequency bands are representative of the hardening process of the cement paste or the time invariant behavior of aggregates, then a comparison between the total energy of the signal and the energy of cement paste and aggregates must present a similar behavior of attenuation described in previous works [18, 19, 25]. This comparison was made possible by modifying Eq. (4) as follows.

$$\alpha_{CP} = -\frac{20}{185} log\left(\frac{E_{CP}}{E_o}\right) \quad (5)$$

$$\alpha_A = -\frac{20}{185} log\left(\frac{E_A}{E_o}\right) \quad (6)$$

where α_{CP} and α_A are the cement paste and aggregates attenuation, respectively. E_{CP} and E_A is the energy of the cement paste and aggregate frequency bands, respectively. E_o is the total energy of the signal and the mean length of the specimens were 185 mm.

3.3. Wavelength analysis

The wavelength λ depends on wave velocity (*UPV)* and transducer frequency (*Ω)* according to

$$\lambda = \frac{UPV}{\Omega} \quad (7)$$

The size of discontinuities in concrete detected by ultrasound signals depends on its wavelength [26]. The sensitivity for detecting a discontinuity of a given size increases with higher frequencies as the wavelength decreases, assuming constant *UPV*. Concrete contains approximately 65 – 70 % of aggregates and 30 – 35% of cement paste by volume. This generates a thin and continuous layer of cement paste covering and filling the empty spaces among aggregates. Therefore, the wavelengths produced by low frequency transducers are more sensitive for detecting aggregates than cement paste, in contrast to high frequency transducers, which preferentially detect cement paste.

For the case of concrete, the ratio of transducer diameter (D) to the wavelength of the transmitted wave (λ) can be used to determine the radiation pattern (β) of the stress pulse in concrete, according to [27],

$$\beta = \frac{D}{\lambda} \quad (8)$$

Most of the energy transmitted into the test specimen is contained within a cone-shaped region that has its base at the transducer surface and its highest amplitude in the normal direction of the transducer surface. The radiation pattern for each transducer, as well as its diameter are shown in Table 2. The radiation pattern mainly influences the wave reflection from the boundaries of the specimen. In our experiments, as the β index increases, it is expected that the wave reflected from boundaries of the specimen would decrease, as well as its influence on the received signal. This influence diminishes even more for higher frequencies due to the high attenuation of concrete [19]. However, further studies on the effect of radiation pattern on our experiments, under similar conditions, are necessary.

4. Results and discussion

4.1. Frequency-domain identification of aggregates and cement paste

Some typical results on the identification of frequencies related to cement paste and aggregates are shown in Figs. 2 to 5. The rest of the figures are found in appendix A. The frequencies associated with cement paste or aggregates are those with amplitudes higher than zero in the corresponding testing age-frequency plots. The close proximity of characteristic frequency bands of cement paste and aggregates can be explained by similar values of the modulus of elasticity of limestone aggregates (10.8 GPa) [28] and cement paste with a w/c = 0.60 (13.38 GPa) [29]. This property has a significant influence on the ultrasonic response of any material, especially for those subjected to longitudinal waves. The response obtained from transducers with the same frequency

but with different types of wave, show that the response of a transversal wave has a better definition of the frequency bands related to cement paste and aggregates, as can be seen by comparing Figs. 2 to 5.

4.2. Estimation of energy evolution over time of selected frequency bands for aggregates and cement paste

It is expected that the energy associated with aggregates remains constant in time, while the energy related to cement paste is assumed to increase, according to the changes in its compressive strength or density. Fig. 6 (transversal wave transducers) and Fig. 7 (longitudinal wave transducers) present the evolution in time of energies produced by different frequency transducers and types of waves. The energies are calculated for the identified frequency bands and are related to the cement paste and to the aggregates. In Fig. 6a, it is shown that for the 50 kHz transducers, the energy associated with aggregates is higher than that associated with cement paste, in contrast to the other frequencies shown in the same figure. There it is shown that, at times no later than 14 days after casting, the energy of cement paste reaches higher values than those values corresponding to aggregates. This behavior may be attributed to the higher value of the wavelength (53 mm at early stages) of the 50 kHz transversal transducer in comparison with the rest of the transducers. As a consequence, the ultrasound waves collect information from larger particles such as aggregates (maximum aggregate size of 13 mm) rather than cement paste in the specimen. This phenomenon is accentuated because concrete is constituted by approximately 65-70% aggregates and 35-30% cement paste by volume, and as wavelength increases with cement paste hardening.

Fig. 7 shows the results for the longitudinal wave transducers. It is observed that the energy associated with cement paste is always higher than the energy of the aggregates after three days of age. This behavior can be attributed to the higher sensitivity of longitudinal waves to changes in density during concrete hardening, in comparison with transversal transducers. This is due to the fact that longitudinal waves which propagate in fluids and solids, have a greater interaction with the cement paste hardening in time, which is reflected in the corresponding energy increase.

4.3. Wave attenuation

The analysis of the attenuation was performed to increase the certainty that the energy bands are in fact related to the hardening process of cement paste and to aggregates.

The attenuation obtained from the energy associated with the frequency bands which were identified as cement paste or aggregates (Fig. 8a) is also consistent with results obtained by previous research [18, 19, 25]. It was found a direct correlation between the addition of aggregates and a higher attenuation of concrete in high frequencies relative to that of cement paste, as opposed to the higher attenuation associated with cement paste in low frequencies. For the longitudinal wave transducers, the resulting attenuation is similar to that obtained for transversal waves in the range of studied frequencies, where the aggregates attenuation is always higher relative to the cement paste attenuation (Fig. 8b).

The attenuation obtained for transversal wave transducers is shown in Fig. 8a, which yielded results as expected [18, 19, 25] with a higher attenuation of cement paste energy than aggregates energy in low frequencies; however, as the frequencies increase, they have a similar behavior until the attenuation of aggregates energy is higher in

comparison with cement paste energy at frequencies corresponding to 500 kHz transversal wave transducer.

In the case of longitudinal wave transducers (Fig. 8b), tested only with high frequencies, an evident attenuation difference between cement paste and aggregates can be appreciated, showing the higher attenuation of the aggregates energy bands in comparison with the cement paste energy bands in every transducer employed.

The average attenuation associated with the hardening of the cement paste for the longitudinal wave transducers is lower than that obtained for the transversal wave transducers. As the energy of frequency bands was used for the estimation of attenuation, due to the propagation properties of the wave, this behavior highlights the higher energy of the cement paste frequency bands obtained with the longitudinal wave transducer. In the case of the aggregates, the average attenuation obtained in 100, 250 and 500 kHz is similar for both wave type transducers.

4.4. Wavelength analysis

Wavelength depends on the frequency and the velocity of the wave Eq. (7). In turn, wave velocity propagation is a function of the properties of the materials such as density (ρ), elastic modulus for longitudinal and shear modulus for transversal waves related to the concrete hardening [30]. These changes in the material are described by different wavelengths which influence the ability to differentiate between cement paste hardening and aggregates [31, 32]. The wavelengths obtained for this experiment are shown in Table 2.

Variations in wavelength for a given frequency, Table 2, are caused by the evolution of the hardening cement paste in concrete. These wavelength values are consistent with the energy behavior presented in Fig. 6 and Fig. 7.

In the case of the 50 kHz transversal wave transducers, produced a higher energy associated with aggregates, than that produced with cement paste (Fig. 6a). This is because of the wavelengths associated with this frequency (56.9 ± 0.22 mm) which have a higher interaction with aggregates (maximum size of 13 mm) than with cement paste, in addition to a higher volume percentage of aggregates in concrete (70%). As a consequence, the attenuation related to the cement paste for this low frequency transducer is high Fig. 8a.

In contrast, the 500 kHz transversal wave transducers, with wavelengths of 3.6 ± 0.02 mm, produce a higher energy associated with cement paste than with aggregates (Fig. 6e) resulting in an opposite attenuation behavior. The rest of the frequencies (Figs. 6b - 6d) present a transitional behavior between these two extremes. The resulting attenuation behaviors (Fig. 8a) are consistent with previous works [18, 19, 25]. Additionally, the sensitivity of transversal wave transducers can be considered to remain constant through evaluation days as shown in the corresponding standard deviation (Table 2).

Regarding the longitudinal waves, the increase in wavelength in comparison with transversal waves, is directly proportional to their higher velocity [33] assuming a constant frequency Eq. (7). This increase is more remarkable at late ages in 250 kHz and 500 kHz frequency transducers and proportional to their standard deviations (Table 2). The constant sensitivity of transversal wave transducer allows a better evaluation of

the hardening process of the cement paste at late ages in contrast to the sensitivity of longitudinal wave which decreases in time proportional to their standard deviations, especially at high frequencies such as 500 kHz.

The wavelength of the longitudinal wave transducers employed (100 – 500 kHz) is similar to those wavelengths corresponding to transitional attenuation behavior obtained for 100 – 250 kHz transversal wave transducers (Table 2 and Fig. 8a). Therefore, the attenuation behavior of longitudinal waves is inconsistent with previous works [18, 19, 25], however if higher and lower frequencies are employed, the attenuation behavior is expected to be consistent.

5. Conclusions

Analysis of the results in the present paper allows for the following conclusions:

(1) The proposed signal analysis procedure allows for the identification of frequency bands related to cement paste and aggregates, whose assumed behavior in time is depicted by the evolution of compressive strength and a constant function, respectively. The attenuation analysis of frequency bands associated with cement paste and aggregates is consistent with previous research.

(2) In this study, due to their high correlation, UPV might be used to describe the behavior associated with cement paste instead of the actual compressive strength.

(3) Transversal wave transducers (especially at 250 kHz) allow for a better definition of the frequency bands associated with the cement paste and

aggregates. In addition, there is a higher correlation with attenuation in comparison with the longitudinal wave transducers.

(4) During the hydration of concrete, the smaller variations in the wavelength of transversal waves provide a higher sensitivity for detecting frequency bands associated with cement paste and aggregates in comparison with those obtained for longitudinal waves.

Future work

Research is under way aimed to improve non-destructive assessment of compressive strength by applying the method outlined in this paper. It will also be applied for detecting chemical reactions that only occur in the cement paste caused by aggressive species such as chloride ions and carbon dioxide.

Acknowledgements

Mario F. Cosmes-López acknowledges the support granted by CONACyT - Mexico and the PIFI program from Instituto Politecnico Nacional for his PhD studies. Francisco Castellanos acknowledges both CONACyT - Mexico and SIP-Instituto Politecnico Nacional for funding the projects ID code CB-154552 and 20140182, respectively. The authors acknowledge Professor George Haley for his English language edition of this manuscript.

References

[1] J. H. Bungey, The validity of ultrasonic pulse velocity testing of in-place concrete for strength, NDT&E Int. 13 (1980), 296-300.

[2] S. Popovics, J.L. Rose, J.S. Popovics, The behaviour of ultrasonic pulse in concrete, Cem. Concr. Res. 20 (1990), 259–270.

[3] J. Hoła, K. Schabowicz, State-of-the-art non-destructive methods for diagnostic testing of building structures – anticipated development trends, Archives of Civ. Mech. Eng. 10 (2010), 5–18.

[4] E.A. Whitehurst, Evaluation of concrete properties from sonic tests, first ed., Purdue Engineering Experiment Station, Michigan, 2011.

[5] G. Trtnik, M. Gams, Recent advances of ultrasonic testing of cement based materials at early ages, Ultrasonics 54 (2014), 66-75.

[6] V.R. Sturrup, F.J. Vecchio, H. Caratin, Pulse Velocity as a Measure of Concrete Compressive Strength, Am. Concr. Inst. 82 (1984), 201-228.

[7] A. Galan, Combined ultrasound methods of concrete testing, NDT&E Int. 30 (1997), 262-262.

[8] M.P. Ismail, K.M. Yusof, A.N. Ibrahim, A combined ultrasonic method on the estimation of compressive concrete strength, INSIGHT 38 (1996), 781–785.

[9] M.F. Kaplan, The effects of age and water to cement ratio upon the relation between ultrasonic pulse velocity and compressive strength of concrete, Mag. Concr. Res. 11 (1959), 85-92.

[10] V. Métaisa, M. Chekroun, L. Le Marrec, A. Le Duffb, G. Plantierb, O. Abrahama, Influence of multiple scattering in heterogeneous concrete on results of the surface wave inverse problem, NDT&E Int. 79 (2016) 53–62.

[11] W. Punuraia, J. Jarzynskib, J. Qub, K. E. Kurtisa, L. J. Jacobs, Characterization of entrained air voids in cement paste with scattered ultrasound, NDT&E Int. 39 (2006) 514–524.

[12] J.H. Kim, H.G. Kwak, J. Min, Characterization of the crack depth in concrete using self-compensating frequency response function, NDT&E Int. 43 (2010), 375–384.

[13] H.J. Yim, H.G. Kwak, J.H. Kim, Wave attenuation measurement technique for nondestructive evaluation of concrete, NDT&E Int. 27 (2012), 81–94.

[14] S.F. Selleck, E.N. Landis, M.L. Peterson, Shah S.P., Achenbach J.D., Ultrasonic investigation of concrete with distributed damage, Am. Concr. Inst. 95 (1998), 27–36.

[15] P.B. Nagy, Fatigue damage assessment by nonlinear ultrasonic materials characterization, Ultrasonics 36 (1998), 375–381.

[16] I. Gabrijel, D. Mikulić, B. Milovanović, Application of ultrasonic measurements for determination of setting and hardening in cement paste, J. Civ. Eng. Architecture 53 (2011), 278–283.

[17] S. Sharmaa, A. Mukherjee, Ultrasonic guided waves for monitoring the setting process of concretes with varying workabilities, Constr. Build. Mater. 72 (2014), 358-366.

[18] E.N. Landis, S.P. Shah, Frequency-dependent stress wave attenuation in cement-based materials, J. Eng. Mech. 121 (1995), 737–743.

[19] T.P. Philippidis, D.G. Aggelis, Experimental study of wave dispersion and attenuation in concrete, Ultrasonics 43 (2005), 584–595.

[20] G. Trtnik, M. Gams, The use of frequency spectrum of ultrasonic P-waves to monitor the setting process of cement pastes, Cem. Concr. Res. 43 (2013), 1–11.

[21] ASTM C31 / C31M-15ae1, Standard Practice for Making and Curing Concrete Test Specimens in the Field, ASTM International, West Conshohocken, PA, 2015

[22] P. Duhamel, M. Vetterli, Fast fourier transforms: A tutorial review and a state of the art, Signal Processing 19 (1990), 259-299.

[23] ASTM C39/C39M-16 Standard Test Method for Compressive Strength of Cylindrical Concrete Specimens, ASTM International, West Conshohocken, PA, 2016

[24] P. Anugonda, J. S. Wiehn, J. A. Turner, Diffusion of ultrasound in concrete, Ultrasonics 39 (2001), 429–435.

[25] A. Villarreal, S. Solis-Najera, L. Medina-Gómez, Application of Waterman-Truell and the Dynamic Generalized Self-consistent Models on Concrete, Physics Procedia 70 (2015), 437 – 441.

[26] J. F. Chaix, V. Garnier, G. Corneloup, Ultrasonic wave propagation in heterogeneous solid media: Theoretical analysis and experimental validation, Ultrasonics 44 (2006), 200–210.

[27] V. M. Malhotra, N. J. Carino, Handbook on Nondestructive Testing of Concrete, second ed., CRC press, Washington, D.C., 2003.

[28] T. Parenta, N. Domedea, A. Selliera, L. Mouattb, Mechanical characterization of limestone from sound velocity measurement, Int. J. of Rock Mech. & Min. Sci. 79 (2015), 149–156.

[29] I. Fischer, B. Pichler, E. Lach, C. Terner, E. Barraud, F. Britzb, Compressive strength of cement paste as a function of loading rate:

Experiments and engineering mechanics analysis, Cem. Concr. Res. 58 (2014), 186–200.

[30] C. Kohlhauser, C. Hellmich, Ultrasonic contact pulse transmission for elastic wave velocity and stiffness determination: Influence of specimen geometry and porosity, Eng. Struct. 47 (2013), 115–133.

[31] B. C. Kim, J. Y. Kim, Characterization of ultrasonic properties of concrete, Mech. Res. Commun. 36 (2009), 207–214.

[32] J. Berriman, P. Purnell, D.A. Hutchins, A. Neild, Humidity and aggregate content correction factors for air-coupled ultrasonic evaluation of concrete, Ultrasonics 43 (2005), 211–217.

[33] S. A. Abo-Qudais, Effect of concrete mixing parameters on propagation of ultrasonic waves, Constr. Build. Mater. 19 (2005), 257-261.

Figure captions

Fig 1. Evolution of concrete compressive strength (blue triangle) and saturated density (green squares) versus age of concrete w/c = 0.60.

Fig. 2. Frequencies versus testing age for (a) aggregate and (b) cement paste. The transducers used were 100 kHz longitudinal wave.

Fig. 3. Frequencies versus testing age for (a) aggregate and (b) cement paste. The transducers used were 100 kHz transversal wave.

Fig. 4. Frequencies versus testing age for (a) aggregate and (b) cement paste. The transducers used were 250 kHz longitudinal wave.

Fig. 5. Frequencies versus testing age for (a) aggregate and (b) cement paste. The transducers used were 250 kHz transversal wave.

Fig. 6. Evolution in time of energies associated with cement paste and aggregates versus testing age for transversal wave transducers (a) 50 kHz, (b) 100 kHz, (c) 180 kHz, (d) 250 kHz and (e) 500 kHz

Fig. 7. Evolution in time of energies associated with cement paste and aggregates versus testing age for longitudinal wave transducers (a) 100 kHz, (b) 250 kHz and (c) 500 kHz

Fig. 8. Attenuation related to cement paste and aggregates energy bands, for (a) transversal and (b) longitudinal wave transducers

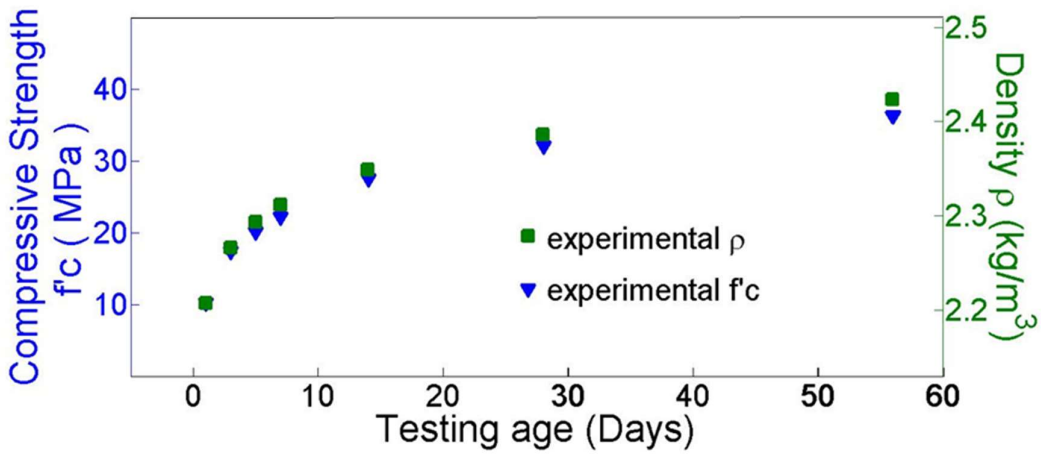
Compressive Strength
f'c (MPa)
Density ρ (kg/m3)
Testing age (Days)
experimental ρ
experimental f'c
10
20
30
40
2.2
2.3
2.4
2.5
0
10
20
30
40
50
60

Fig 1.

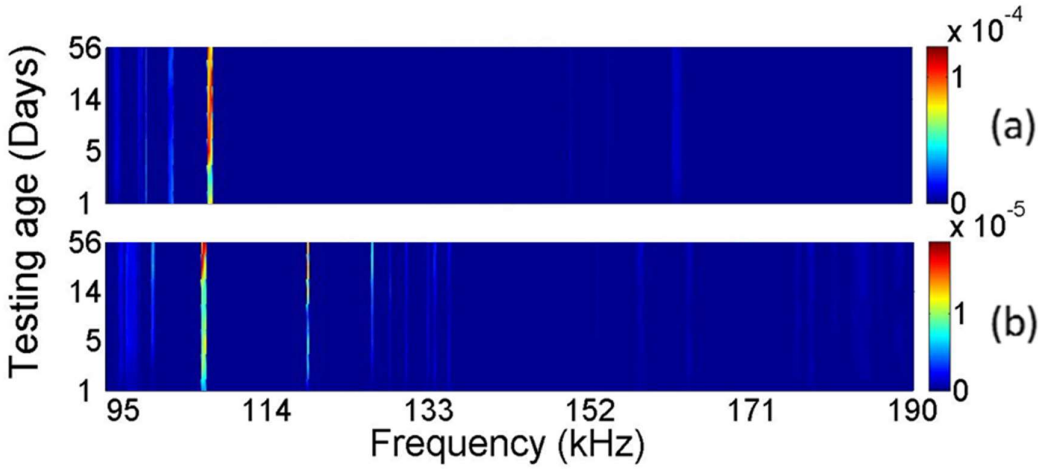
Testing age (Days)
56
14
5
1
x 10^-4
1
0
(a)
x 10^-5
(b)
95
114
133
152
171
190
Frequency (kHz)

Fig. 2.

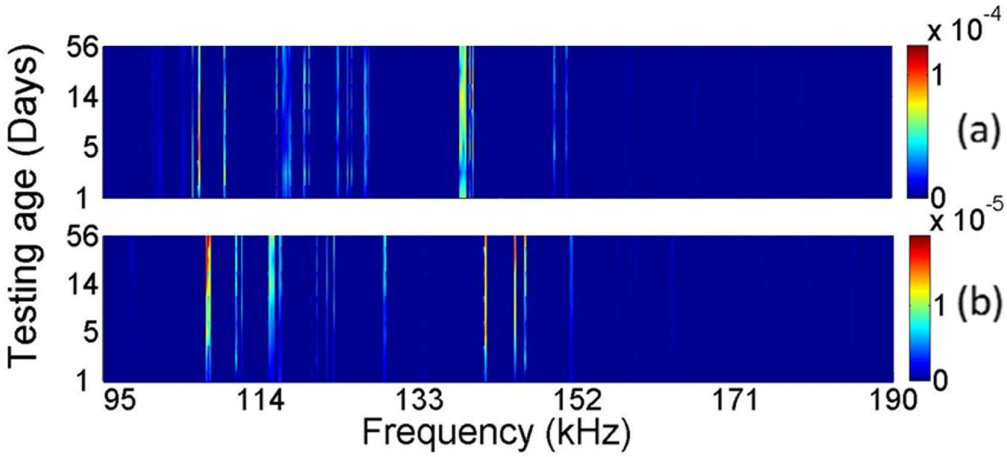
Testing age (Days)
56
14
5
1
x 10^-4
1
(a)
0
x 10^-5
1
(b)
0
95
114
133
152
171
190
Frequency (kHz)

Fig. 3.

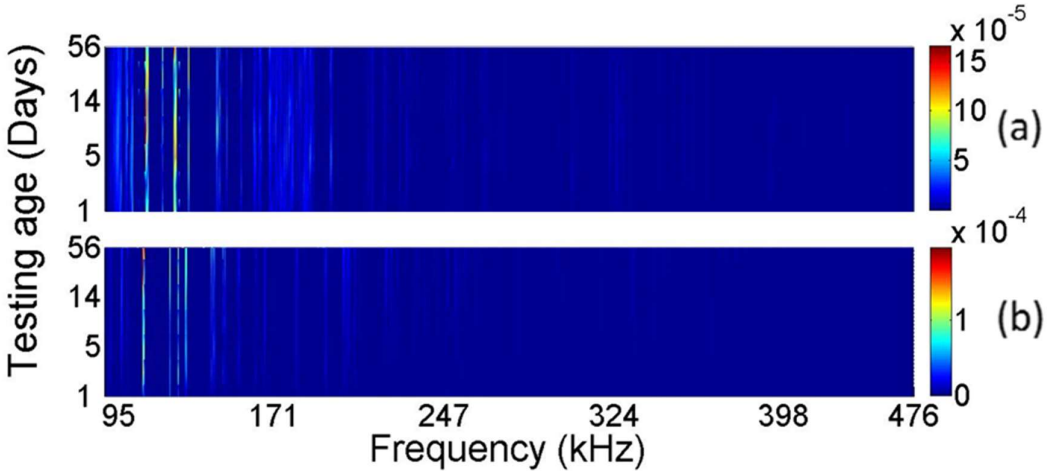
Testing age (Days)
56
14
5
1
x 10^-5
15
10
5
(a)
x 10^-4
1
0
(b)
95
171
247
324
398
476
Frequency (kHz)

Fig. 4.

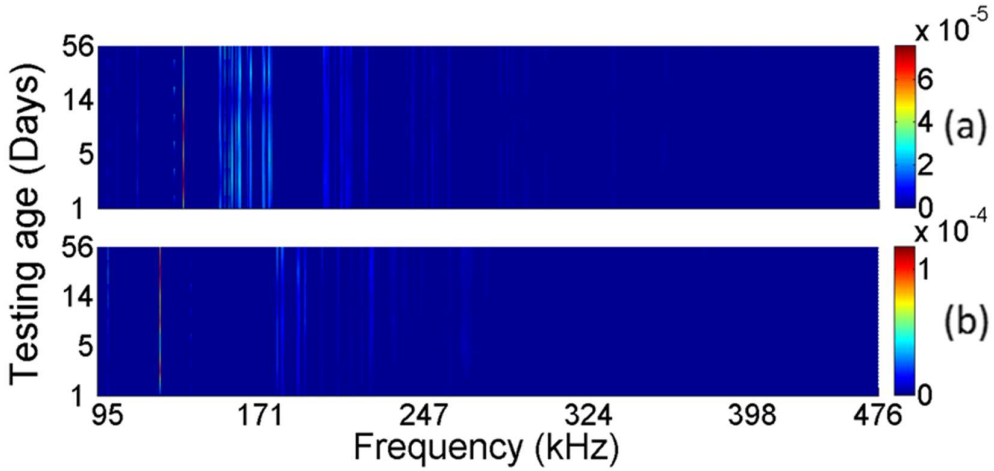
Testing age (Days)
56
14
5
1
x 10^-5
6
4
2
0
(a)
x 10^-4
1
0
(b)
95
171
247
324
398
476
Frequency (kHz)

Fig. 5.

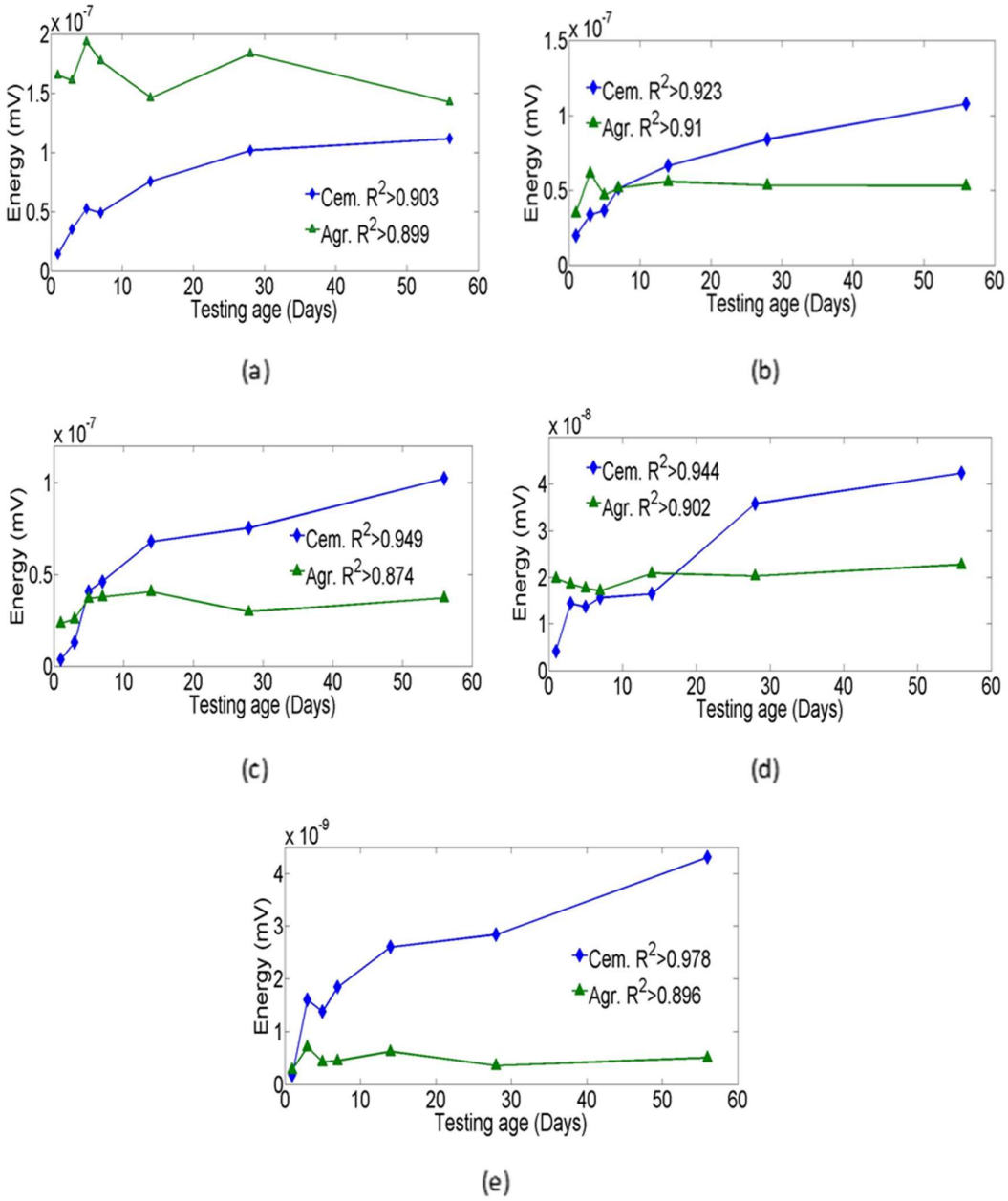
x 10^-7
Energy (mV)
Testing age (Days)
Cem. R^2>0.903
Agr. R^2>0.899
(a)
x 10^-7
Energy (mV)
Testing age (Days)
Cem. R^2>0.923
Agr. R^2>0.91
(b)
x 10^-7
Energy (mV)
Testing age (Days)
Cem. R^2>0.949
Agr. R^2>0.874
(c)
x 10^-8
Energy (mV)
Testing age (Days)
Cem. R^2>0.944
Agr. R^2>0.902
(d)
x 10^-9
Energy (mV)
Testing age (Days)
Cem. R^2>0.978
Agr. R^2>0.896
(e)

Fig. 6.

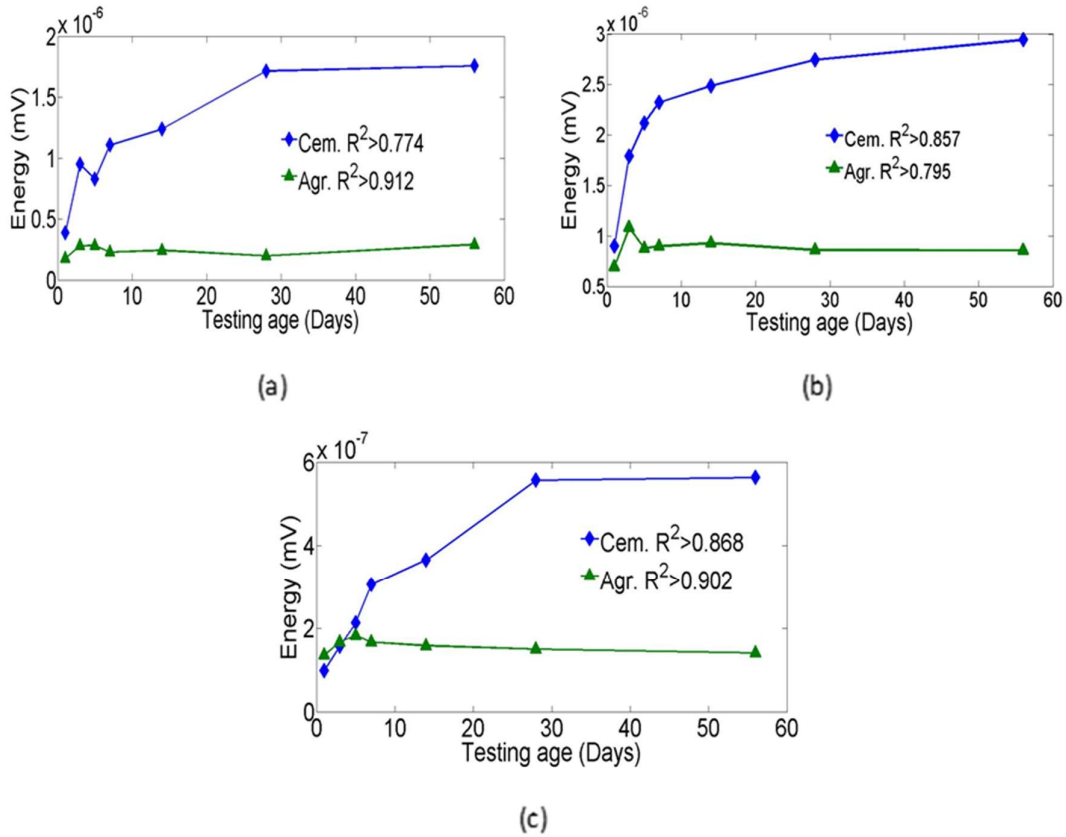
x 10^-6
Energy (mV)
Testing age (Days)
Cem. R^2>0.774
Agr. R^2>0.912
(a)
x 10^-6
Energy (mV)
Testing age (Days)
Cem. R^2>0.857
Agr. R^2>0.795
(b)
x 10^-7
Energy (mV)
Testing age (Days)
Cem. R^2>0.868
Agr. R^2>0.902
(c)

Fig. 7.

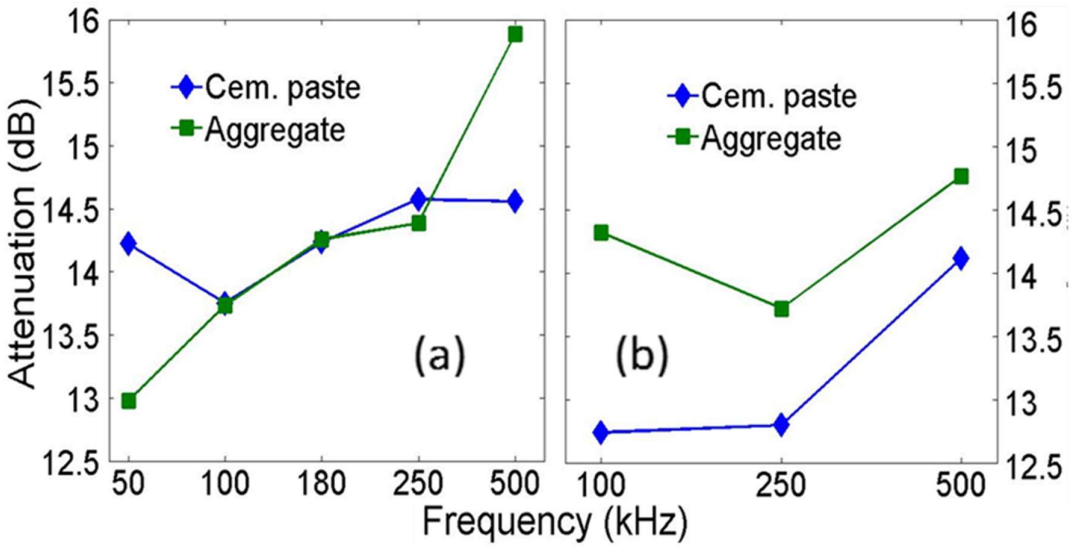
Attenuation (dB)
16
15.5
15
14.5
14
13.5
13
12.5
Cem. paste
Aggregate
(a)
(b)
50
100
180
250
500
100
250
500
Frequency (kHz)

Fig. 8.

Table 1. Chemical composition of main oxides for the Ordinary Portland Cement (OPC) used.

Main oxides components	**%**
SiO_2	21.1
Al_2O_3	3.7
Fe_2O_3	4.5
CaO	61.9
MgO	1.8
K_2O	0.3
Na_2O	0.1
SO_3	1

Table 2. Wavelengths generated by the time-evolution of specimens, using the ultrasonic pulse velocity of each transducer

Transducer frequency (kHz)	**Transducer diameter (D) (mm)**	**wavelength at day 1 (λ) (mm)**	**wavelength at day 56 (λ) (mm)**	**Mean ± std dev wavelength (λ_M) (mm)**	**Radiation pattern $\beta = \frac{D}{\lambda_M}$**
		Transversal wave transducer			
50	42	53.2	60.0	56.9 ± 2.29	0.7
100	29	21.6	25.7	24.2 ± 1.56	1.2
180	42	13.7	13.5	13.6 ± 0.13	3.1
250	29	6.5	7.8	7.3 ± 0.42	4.0
500	29	3.2	3.8	3.6 ± 0.21	8.1
		Longitudinal wave transducer			
100	42	22.5	28.5	25.5 ± 2.19	1.6
250	42	15.5	19.1	17.4 ± 1.51	2.4
500	29	7.3	10.1	9 ± 0.95	3.2

Appendix A

Fig. 9. Frequencies versus testing age for (a) aggregate and (b) cement paste. The transducers used were 50 kHz transversal wave.

Fig. 10. Frequencies versus testing age for (a) aggregate and (b) cement paste. The transducers used were 180 kHz transversal wave.

Fig. 11. Frequencies versus testing age for (a) aggregate and (b) cement paste. The transducers used were 500 kHz longitudinal wave.

Fig. 12. Frequencies versus testing age for (a) aggregate and (b) cement paste. The transducers used were 500 kHz transversal wave.

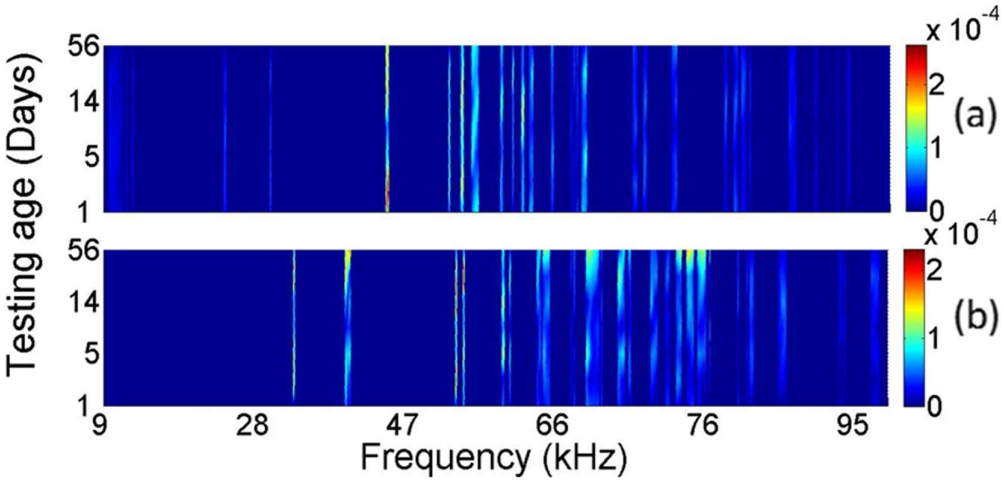
Testing age (Days)
56
14
5
1
x 10^-4
2
1
0
(a)
(b)
9
28
47
66
76
95
Frequency (kHz)

Fig. 9.

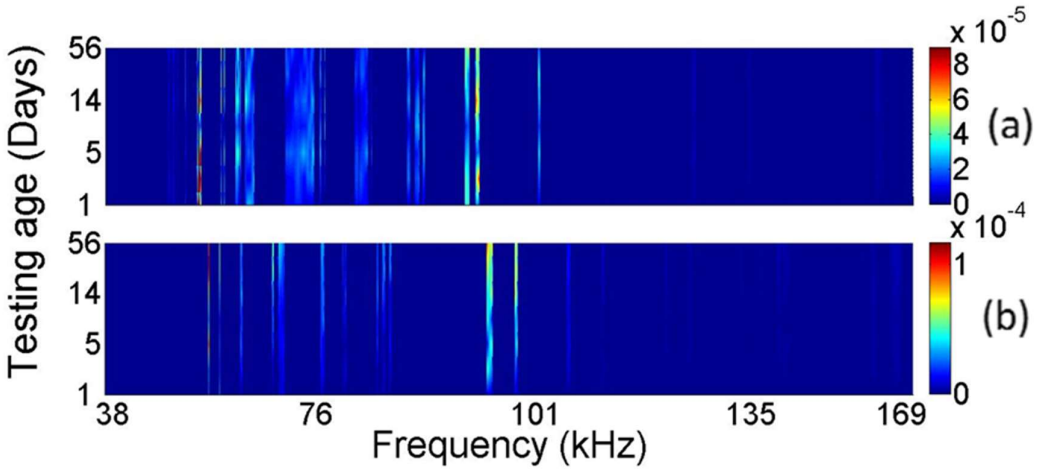
Testing age (Days)
56
14
5
1
x 10^-5
8
6
4
2
0
(a)
x 10^-4
1
0
(b)
38
76
101
135
169
Frequency (kHz)

Fig. 10.

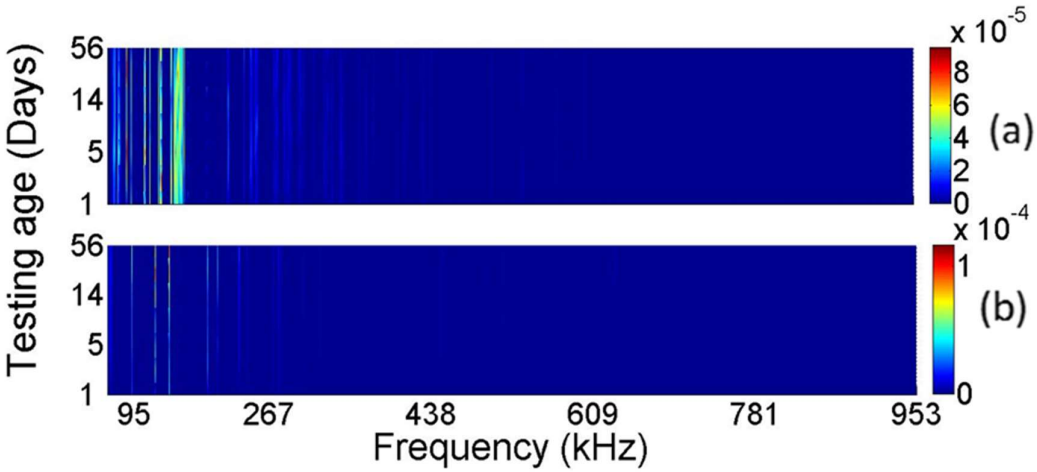
Testing age (Days)
56
14
5
1
x 10^-5
8
6
4
2
0
(a)
x 10^-4
1
0
(b)
95
267
438
609
781
953
Frequency (kHz)

Fig. 11.

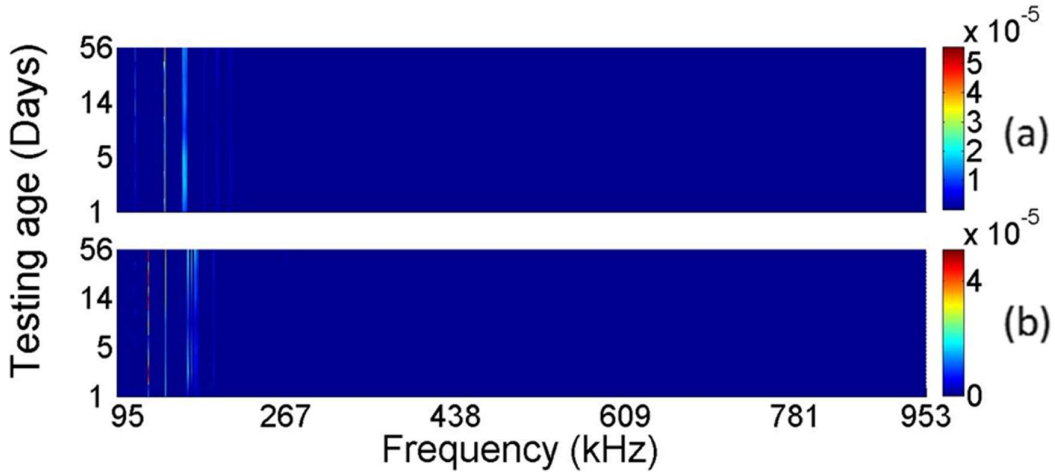
Testing age (Days)
56
14
5
1
x 10^-5
5
4
3
2
1
(a)
56
14
5
1
x 10^-5
4
0
(b)
95
267
438
609
781
953
Frequency (kHz)

Fig. 12.

Capítulo II

Non-destructive ultrasound based cement paste carbonation index

Mario F. Cosmes-López[1], Francisco Castellanos[2*], Prisciliano F. de J. Cano-Barrita[2], Frank M. León-Martínez[2]

[1] *PhD student at Instituto Politecnico Nacional, CIIDIR Unidad Oaxaca, Hornos No. 1003, Santa Cruz Xoxocotlán, Oaxaca, Mexico, C.P. 71230.*

[2] *Researcher at Instituto Politecnico Nacional, CIIDIR Unidad Oaxaca, Hornos No. 1003, Santa Cruz Xoxocotlán, Oaxaca, Mexico, C.P. 71230.*

Phone: + 52 951 5170610, Emails: mcosmesl1200@alumno.ipn.mx, fcastellanos@ipn.mx, pcano@ipn.mx and fmleonm@ipn.mx

*Corresponding author

Abstract

This study presents a new method to assess the degree of carbonation in cement paste specimens, by analyzing their ultrasound response to different excitation frequencies. Eighteen cylindrical cement paste specimens measuring 50 mm in diameter and 57 mm in height were cast with three different water to cement ratios (w/c = 0.60, 0.50 and 0.40). The samples were moist cured for four months to reach a high degree of hydration. Then the samples were conditioned in an environmental chamber at 30 ºC and 65 % relative humidity. After obtaining constant mass, each specimen was coated with epoxy resin on the curved surface, one circular face was covered with parafilm. The specimens were then exposed to accelerated carbonation in an environmental chamber at 30 ºC, 65 % relative humidity, and 4 % CO_2 (v/v). One control specimen was kept at the same environmental conditions of temperature and relative humidity, without CO_2. All the specimens were tested at 1, 3, 5, 7, 14, 28 and 56 days, during carbonation process, using longitudinal and transversal ultrasonic waves with frequencies ranging from 100 kHz to 500 kHz. Assuming the carbonation in cement paste causes changes in the frequencies spectrum as the carbonation front progresses, causing important changes on porosity and pore structure of the cement paste. By analyzing these changes, we may infer the degree of carbonation in the specimen. Results show that it was possible to assess the degree of carbonation of cement paste specimens by frequency domain analysis as a function of carbonation time, regardless of the water to cement ratio.

Keywords: ultrasound analysis; carbonation; cement paste; Fourier analysis; carbonation index

1. Introduction

The alkaline pore solution of the hydrated cement paste protects the reinforcing steel from corrosion caused by carbonation [1,2]. Carbonation is the result of the reaction between CO_2 from the environment and the main hydration products such as calcium hydroxide and CSH in the presence of moisture, generating calcium carbonate and silica gel [3]. As a result, the pH of the pore solution is reduced from above 12.5 to less than 9. This may destroy the passivating layer on the steel and corrosion starts [4]. Carbonation not only affects the chemistry of the pore solution, but also affects the porosity and pore size distribution of the cement paste [5]. In some cases, the porosity is reduced and the strength is increased. In other cases, the porosity is increased, especially when using fly ash [6].

Penetration of CO_2 is function of the permeability of hardened cement paste in concrete, as well as the CO_2 concentration and environmental factors such as temperature and relative humidity [7]. The carbonation front follows the square root of time behavior. Regarding the environmental factors, the penetration is strongly influenced by the concentration of CO_2, temperature and relative humidity [8]. Therefore, conclusions based on accelerated carbonation tests, can be used to estimate the service life of reinforced concrete structures [6, 9].

The most common and simple technique used to measure the carbonation depth is by spraying a phenolphthalein indicator on a freshly broken surface. However, it is destructive in nature and in addition it underestimates the carbonation front penetration [10]. Other destructive methods such as the thermogravimetric analysis (TGA), X-Ray diffraction and Fourier transformation infrared spectroscopy (FTIR) have been also used to detect the changes in concrete produced by

carbonation [11,12,13]. The gammadensimetry [14] is able to measure the total penetration of the CO_2 during laboratory accelerated tests. However, in order to obtain a full picture of the carbonation process numerous samples need to be tested.

Transmission wave velocity and wave attenuation are affected by the density and the elastic modulus of materials [15,16], which makes ultrasound wave analysis a potential technique for assessing carbonation of the cement paste. This article presents a new approach on the analysis of ultrasound signals to study carbonation of mature cement paste specimens with different w/c ratios. This approach was adapted from our methodology proposed for distinction of aggregate and cement paste in concrete samples from analysis of ultrasound signals [17].

2. Experimental procedure

2.1. Materials

Mexican ordinary Portland cement class 30RS (ASTM C150 Type I) was used. A total of 18 cylindrical cement paste specimens measuring 50 mm in diameter and 57 mm in height were cast with three different w/c ratios of 0.60, 0.50 and 0.40. After one day, the specimens were stripped and moist cured in a saturated lime solution at 40 ± 2 °C for four months, according to the ASTM C31 [18]. Then the specimens were stabilized in an environmental chamber at 30 ºC and 65 % relative humidity, until constant mass was achieved.

After stabilization, each specimen was coated with epoxy resin on the curved surface. Before carbonation commenced, one circular face was covered with paraffin film to expose only one face to CO_2 penetration. Five specimens of each w/c ratio were exposed to accelerated

carbonation in an environmental chamber at 30 ºC, 65 % relative humidity, and 4 % CO_2 (v/v). One control specimen was kept at the same temperature and relative humidity, without CO_2.

2.2. Method

2.2.1. Ultrasonic measurements

Six specimens were tested at ages of 1, 3, 5, 7, 14, 28 and 56 days, after beginning the carbonation process. For each test, the ends of each specimen were covered with paraffin film and heated with a heat gun for 60 seconds in order to obtain a smooth thin layer, which prevented penetration of the coupling agent (petroleum jelly) into the specimen. The excitation signal was generated by a 5077PR pulser/receiver with a voltage of 200 V and a variable factor of electronic damping or gain depending on the amplitude of the received signal. A record was maintained of their responses in through-transmission with longitudinal and transversal ultrasonic waves, generated by transducers with frequencies ranging from 100 kHz to 500 kHz. The position of the transducers and their applied pressure were kept constant during the experiment.

2.2.2. FTIR measurements

Three specimens of each w/c ratio were taken at 1, 3, 5, 7, 14, 28 and 56 days, for carbonated and control specimens. Once the epoxy resin coat was removed, the cement paste samples were crushed with hammer and chisel and then the small pieces were ground with an agate mortar. The fine powder obtained was sieved by the No. 100 mesh (150 μm), then oven-dried at 105 ° C for 24 hours, and finally stored in sealed bags. The bags were inside a desiccator with silica gel and soda lime at room temperature, to avoid moisture adsorption and carbonation of the powder samples until FTIR measurements were performed [13].

Three different FTIR spectra of each powder sample were taken with a ThermoScientific instrument Model Nicolet 6700 (ThermoScientific, MA, USA) and the mean value of the area under the curve was calculated for the vibration bands at 1418 cm^{-1} and 872 cm^{-1} corresponding asymmetric stretching and out plane bending for the carbonate ion in the $CaCO_3$. The initial amount of $CaCO_3$ in the anhydrous cement (3%) was determined by thermogravimetric analysis and this value was related to the area under the curve of the bands corresponding to $CaCO_3$ in the FTIR spectrum. This served as a basis for estimation of the amount of $CaCO_3$ by weight in the carbonated samples.

3. Wave analysis

3.1. Signal processing

The method proposed for analysis of the ultrasound signals was intended to assess the degree of carbonation in cement pastes with different w/c ratios. The main feature exploited by the proposed method was that the CO_2 penetration affects the microstructure of the cement paste by generating of calcium carbonate, and the consequent modification of its density and physical properties [19]. Assuming that the degree of hydration [20] of the cement pastes was high because of the relatively long moist curing time, it was feasible to consider that variations in the ultrasonic response of cement pastes will be a result of carbonation, as opposed to the invariant behavior of the control specimens.

This analysis methodology was based on our previous work [17]. The first step in the proposed analysis was to calculate the time-discrete Fourier Transform (TDFT) of the ultrasound signal

$f(n\Delta t)$, according to Eq. (1). The Fast Fourier Transform (FFT) is a standard signal processing technique for analyzing ultrasound signals [21].

$$\mathrm{F}(\mathrm{k}\Delta\omega) = \frac{1}{2\pi}\sum_n f(n\Delta t)e^{-i\left(2\pi kn/N\right)}\Delta t \qquad (1)$$

where T is the duration of the ultrasound signal, discretized at a sampling rate Δt=T/N, and kΔw are the resulting discrete frequencies.

A window of F(kΔω) was subsequently selected from the frequency response function of the transducers with an intensity greater or equal to 6 dB, as specified by the ultrasound transducer manufacturer.

$$\mathrm{G}(\mathrm{k}\Delta\omega) = \begin{cases} F(k\Delta\omega), & k_1 \leq k \leq k_2 \\ 0, & elsewhere \end{cases} \qquad (2)$$

The changes over time of the seven spectra obtained (1, 3, 5, 7, 14, 28 and 56 days) from ultrasound measurements $\mathrm{G_i}(k\Delta\omega)$, where $1 \leq i \leq 7$, was analyzed for the identification of the carbonation process. This analysis consists of the correlation of variations along time of every frequency amplitude $|\mathrm{G_i}(\mathrm{k}\Delta\omega)|$, with a constant function. For the identification of frequencies k_c related to the carbonated cement paste. The correlation was made from the first two testing days, until the eighth day, obtaining seven sets of correlations for each specimen.

A histogram was obtained for each of the seven sets of correlations. The abscissa *x* was discretized by class and associated to each correlation coefficient, for each of the seven sets of correlations. The ordinate represents the number of frequencies in each class. The size of the class was chosen with a precision of 0.001. In order to improve understanding of the data

behavior, the histogram obtained was duplicated using a function which satisfies the next condition:

$$H(x) = H(2 - x) \tag{3}$$

Such that the function obtained is defined as follows:

$$K(x) = \begin{cases} H(x), \ 0 \leq x \leq 1 \\ H(2 - x), \ 1 < x \leq 2 \end{cases} \tag{4}$$

Then, the resulting signal was adjusted to a normal distribution function, minimizing the squared error, as shown in Figure 1.

$$I_a(x) = \beta \, e^{-\left(\frac{x-1}{\sigma}\right)^2} \tag{5}$$

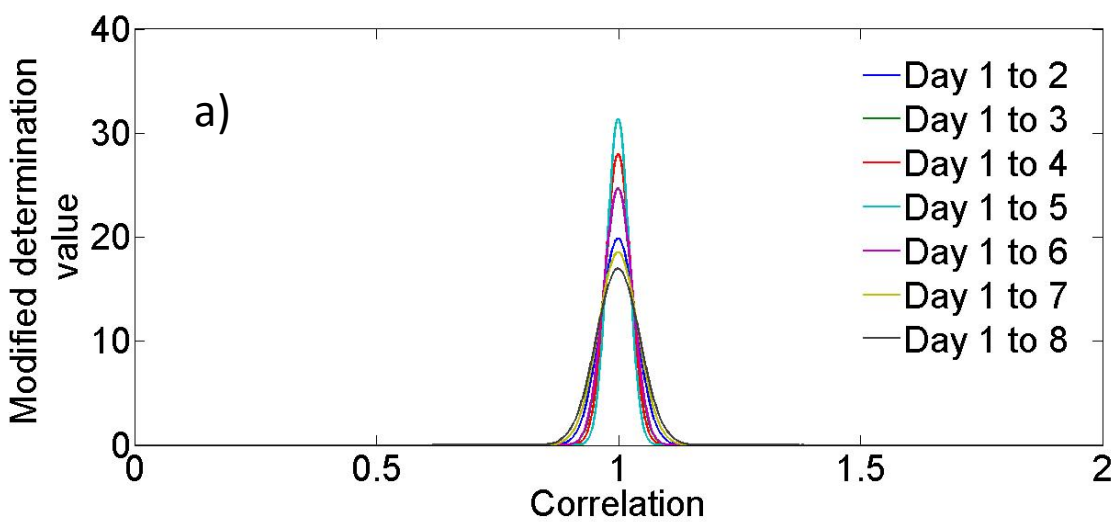

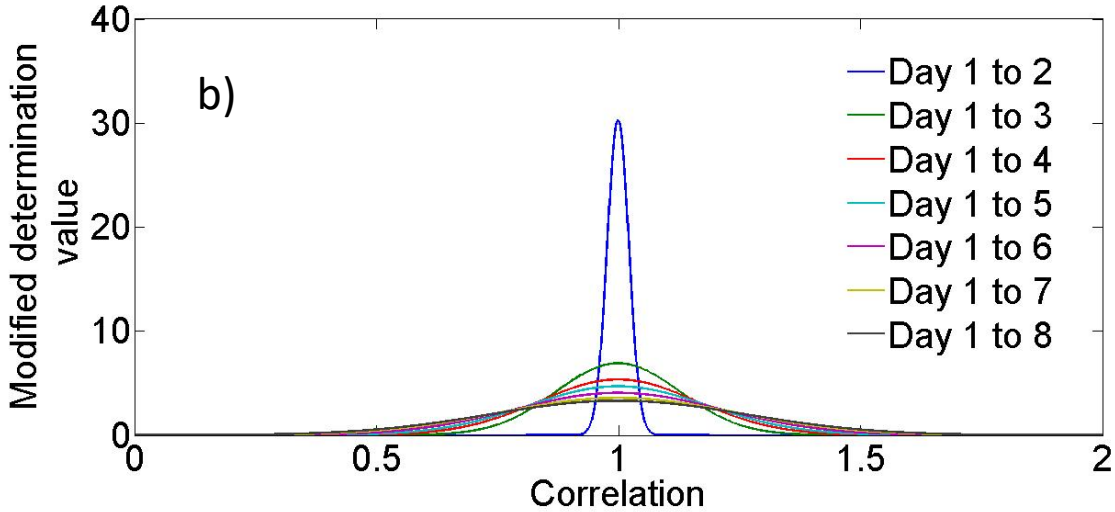

Figure 1 Normal distribution adjustment of the accumulative data for each measurement day, of control (a) and carbonated (b) specimen, for the water to cement ratio of 0.50 using the longitudinal wave transducer of 100 kHz.

This process was performed for each of the seven set of correlations. Using the inverse of the amplitude β, the index I was obtained as follows.

$$I = \frac{(w/c)*\gamma}{\beta} \quad (6)$$

where I is the carbonation index, dependent on the w/c and the empirical obtained factor γ, that may be linked to exposure conditions.

In previous studies, it was found that the exposure to high concentration of CO_2 cause a degradation of the calcium silicate hydrate (C-S-H), weakening the cement matrix which will generate cracks through the specimens, being more evident with higher water/cement ratios [5].

Since the generation of cracks is highly probable when the cement paste is carbonated, as the products generated by the carbonation reaction occupy a higher volume than the hydration products [22, 23]. For this reason, it was necessary to correct the previous index by attenuation A using the following equation.

$$A = -\log\left(\frac{A_E}{A_S}\right) \tag{7}$$

where A_E is the amplitude of the first measurement day and A_S is the amplitude of the subsequent measurement days.

The correction by attenuation Eq. (7) of the index obtained in Eq. (6), produces the index I_A for the carbonation of the cement paste was obtained as:

$$I_A = I - A \tag{8}$$

3.2. Wavelength

The wavelength λ depends on wave velocity (UPV) and transducer frequency (Ω) according to Eq. (9).

$$\lambda = \frac{UPV}{\Omega} \tag{9}$$

The sensitivity to detect defects/changes in the cement paste was given by the relation between the size of the defect/changes and the wavelength [24]. The sensitivity depends on the transducer frequency, which increase directly proportional to the frequency employed, assuming constant

UPV [25]. In carbonated specimens, different degrees of carbonation may be detected depending on the frequency transducers used.

4. Results and discussion

4.1. Ultrasound pulse velocity

The first analysis of the data was calculating the ultrasound pulse velocity (UPV). In Figure 2 it is shown the evolution in time of the UPV for all the specimens with three different w/c ratios. The UPV allows only distinction between the different w/c ratio employed, but not for the difference between control and carbonated specimens.

As can be seen, the standard error of the UPV for the w/c = 0.50 and 0.60 was higher in comparison with that of the w/c = 0.40. This effect may be due to the generation of cracks caused by the carbonation process which was higher for the w/c = 0.50 and 0.60. In the case of the w/c = 0.40 showed an increase of the UPV after 30 days of CO_2 exposure, influenced by the attack of C-S-H and CH producing important changes in the elastic modulus and density, despite of the short carbonation front.

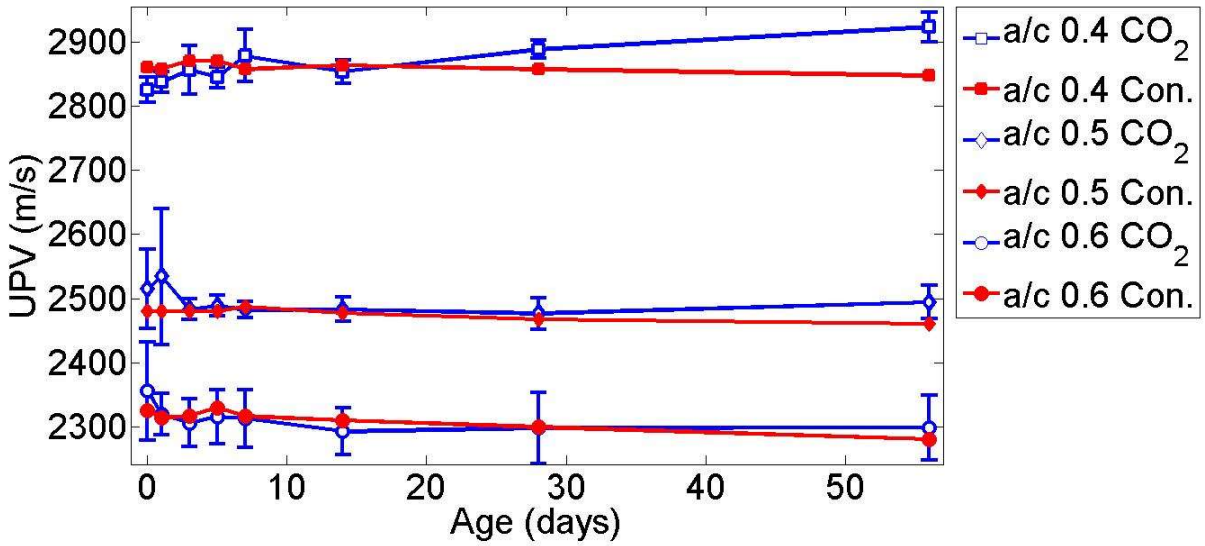

Figure 2. Evolution in time of the UPV versus testing age for control (red lines) and carbonated (blue lines) specimens for water/cement ratios of 0.40 (square), 0.50 (diamonds) and 0.60 (circles). The error bars represent one standard deviation.

Results from ultrasound testing were compared with the content of calcium carbonate ($CaCO_3$) estimated by the Fourier Transform Infrared Spectroscopy (FTIR) measurements [13], presented in the following section.

4.2. Carbonation index

Variations in the porosity and pore structure of cement pastes caused by carbonation depend on the properties of the cement paste and the exposure environmental conditions [19, 27]. Three w/c ratios (0.40, 0.50 and 0.60) were analyzed for indexing the degree of carbonation in cement pastes whose results are shown in Figures 3-5.

It was expected that the progressive changes caused by the carbonation process, gradually modify the cement paste microstructure. These variations slowly affect the frequency of the ultrasound response. This effect distinguishes the control from the carbonated specimens.

4.2.1. Cement paste samples with water/cement ratio of 0.60

Figure 3 shows the results of the ultrasonic measurements for the control and carbonated specimens for cement paste with w/c ratio of 0.60. Figure 3a shows the evolution over time of the carbonation index for the control and carbonated specimen tested with 100 kHz longitudinal wave transducers. The behavior between both types of specimens was similar, although the trend of the carbonation index had a strong correlation with the FTIR data. The behavior of the control specimen may be explained by the stabilization process which cause drying shrinkage and cracking of the cement paste [28]. This was reflected in variations of the ultrasound response of the control specimens during the measurements as had been seen in previous studies [29,25]. This effect was present in the rest of the measurements with other transducers, as can be seen in Figures 3b-e, but with less impact in the index response due to the variations in wavelength calculated in Table 1 [30].

In Figures 3b and 3d, measurements with the 100 kHz and 250 kHz transversal wave transducers, respectively, had a weak correlation with the FTIR data. The former correlation was mostly caused by the cracking and porosity of the specimens with a high w/c ratio [19]. These factors had a high impact on the propagation of transversal waves, making it difficult to assess the carbonation penetration, since they cannot propagate through fluids (water and air) [31].

Figure 3c shows the measurements with the 250 kHz longitudinal wave transducers. The control specimens keep a behavior almost constant in contrast with the index of the carbonated specimen whose values increase. The correlation between the carbonation index proposed and the FTIR data was strong. Although, the correlation was weaker than that obtained with the 100 kHz longitudinal wave transducers, in this case, it was possible to distinguish between the behavior of the control and the carbonated specimen. This distinction was possible due to the changes in wavelength and in the propagation properties of this kind of waves (Table 1) which can travel through solids and fluids [32].

Measurements with the 500 kHz longitudinal wave transducers are shown in Figure 3e. The distinction between control and carbonated specimen behavior was easier, in comparison with the results of the other transducers. Also, the carbonation index had the strongest correlation with the FTIR data and the dispersion of the carbonation specimens was the lowest. The wavelength and the propagation properties of the longitudinal waves of these transducers [33], as shown in Table 1, improves tracking of the carbonation process. Furthermore, the final value of the carbonation index proposed was close to the one obtained with FTIR. However, the losses of energy are so high that causes underestimation of carbonation degree.

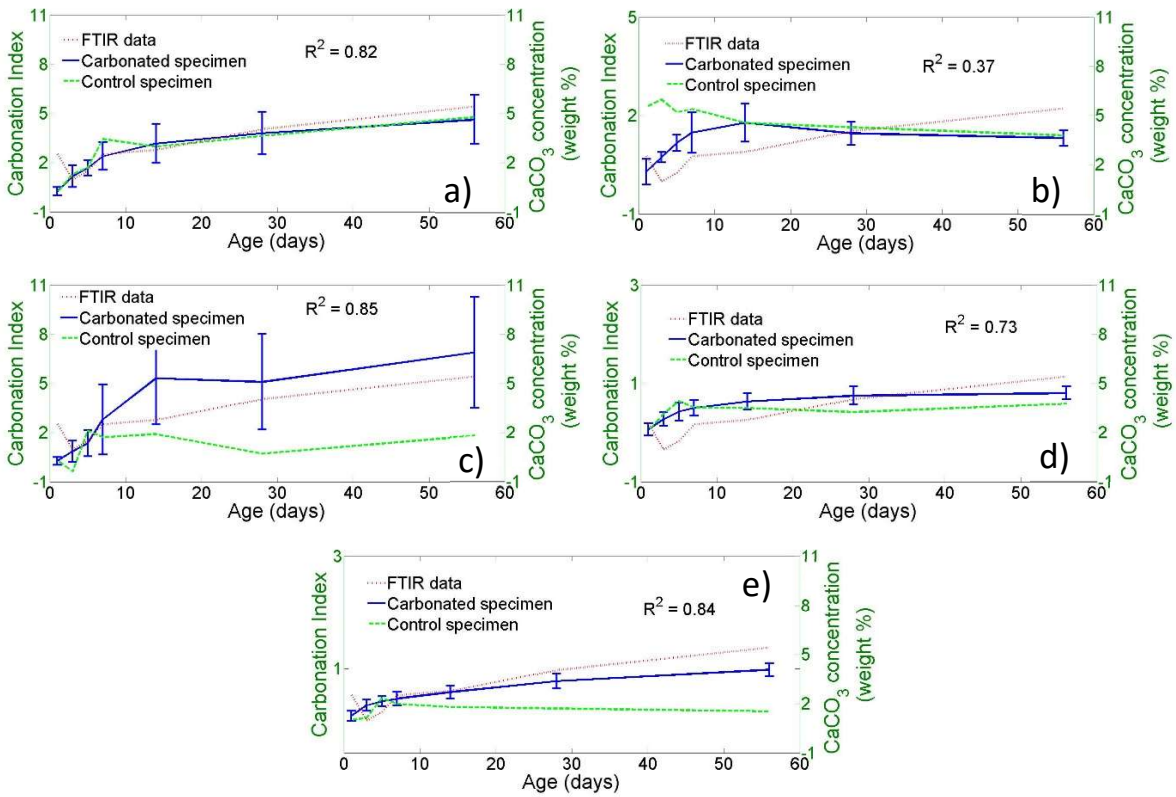

Figure 3. Evolution of carbonation index and content of calcium carbonate by FTIR, versus testing age for longitudinal wave transducers of 100 kHz (a), 250 kHz (c), 500 kHz (e) and transversal wave transducers of 100 kHz (b), 250 kHz (d), for cement paste specimens with w/c ratio = 0.60.

Table 1 shows how the wavelength of the carbonated specimens was lower than the control samples, which is explained by the density increase due to generation of calcium carbonate ($CaCO_3$), for the same frequency of the transducers. As the transducer frequency increases, the wavelength decreases enhancing the sensitivity of the ultrasound signals, along with reducing the standard deviation between specimens. Also, a small decrease between the same frequency transducers but different wave type is produced; this decrease was more visible in carbonated specimens.

Table 1. Mean and standard deviation of the wavelengths generated by the time-evolution of control and carbonated specimens with w/c=0.6

Frequency (kHz)	Diameter of Transducer (D) (mm)	Control wavelength (λ) (mm)		Carbonated wavelength (λ) (mm)	
		Mean ($M_{\lambda Co}$)	Std dev	Mean ($M_{\lambda Ca}$)	Std dev
Longitudinal wave transducer					
100	42	23.13	0.47	23.12	0.15
250	42	9.38	0.31	9.28	0.08
500	29	4.74	0.17	4.68	0.04
Transversal wave transducer					
100	29	22.56	0.66	22.33	0.17
250	29	9.35	0.34	9.21	0.09

4.2.2. Cement paste samples with water/cement ratio of 0.50

Figure 4 shows the results of the ultrasonic measurements for the control and carbonated specimens with a w/c ratio of 0.50. The results of the ultrasound measurements with the 100 kHz transversal wave transducer are shown in Figure 4b. Although, the correlation with the FTIR data was weak, the distinction between the control and the carbonated specimens was possible. This was because of the slow penetration of CO_2, result of the lower permeability of this paste compared with the permeability of the paste with w/c = 0.60 [34].

This decrease in the carbonation ratio allows a slower formation of the $CaCO_3$, enlarging the time of occurrence of the structural changes in the cement paste [19]. These smooth the process of carbonation allowing a better assess of the changes in the cement matrix and therefore a better studied of the specimen, which was reflected in the stronger correlation of the carbonation index for all transducers, in comparison with the cement paste of 0.60. In the case of Figures 4a, 4c, 4d, and 4e, the correlation with the FTIR data becomes stronger as the transducer frequency

increases. This behavior was related to the gain in sensitivity due to the decrease of the wavelength as the transducer frequency increases, as shown in Table 2.

Figure 4a shows the evolution in time of the carbonation index for the 100 kHz longitudinal wave transducers. It was possible to distinguish the behavior between the control and the carbonated cement paste specimens. The correlation was stronger than the 100 kHz transversal wave transducer, which might be explained by fewer losses of the signal energy by cracks, void and water caused by the carbonation process [6]. Nevertheless, the standard error of the data was higher than the ones of Figures 4c, 4d and 4e.

The correlation obtained by the 250 kHz longitudinal wave transducer was the strongest on evaluating the 0.5 w/c cement paste, as shown in Figure 4c. The rise of the correlation was mostly caused by the decrease of the wavelength and the property of the longitudinal waves to travel through different media, as shown in Table 2. This causes less energy losses due to the specimen heterogeneities with better interaction during the measurements, but increasing the standard error between the carbonation index for different specimens, as well as the sensitivity.

The results for the 250 kHz transversal wave transducer are shown in Figure 4d. The stronger correlation, compared with the 100 kHz transversal wave transducer, was due to the lower wavelength. However, the sensitivity was not enough to surpass the correlation of higher or equal longitudinal wave transducers frequency. Although, the preference of the transversal waves to propagate through solids and the slower generation of the solid phases ($CaCO_2$) of the carbonation process had high impact on the standard error of the carbonation index of different specimen measurements, as seen in Figure 4d.

The results for the 500 kHz longitudinal wave transducer are shown in Figure 4e. The correlation with the FTIR data was the second strongest of the transducer measurements, because of the wavelength (Table 2) which allows a better interaction with the specimen recollecting more information of the specimen, also cause a higher loss of energy. As expected, the sensitivity increases with time, but the heterogeneities between different specimens induces a rise of standard error in the carbonation index for different specimens, caused by the heterogeneities produced by the carbonation process.

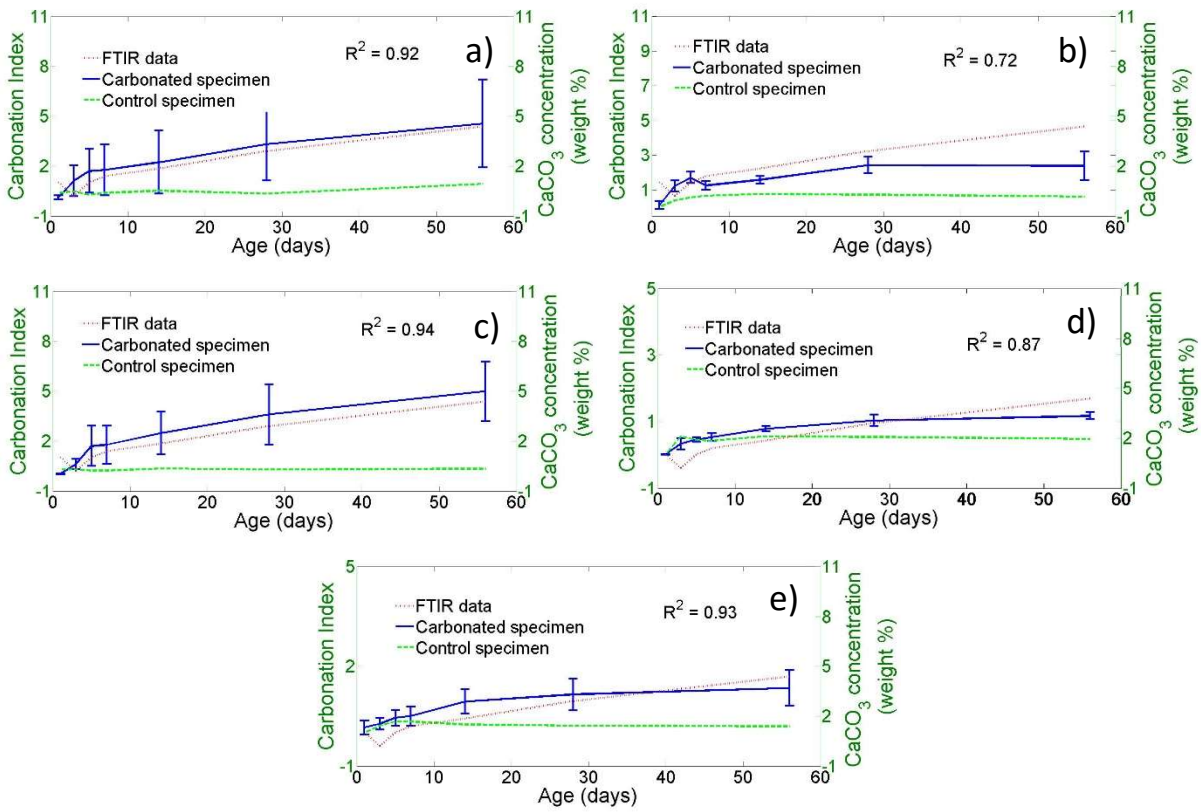

Figure 4. Evolution of carbonation index and content of calcium carbonate by FTIR, versus testing age for longitudinal wave transducer 100 kHz (a), 250 kHz (c), 500 kHz (e) and transversal transducer 100 kHz (b), 250 kHz (d) for cement paste specimens with w/c ratio = 0.50.

As stated, the wavelength decreases as the frequency transducer increases, but the wavelength between control and carbonated specimens was very close one to another, regardless of the transducer frequency. This behavior was due to the slower carbonation reaction process. The decrease between the same frequency but different type of wave was more evident with the 100 kHz transducers than with the 250 kHz transducers.

Table 2. Wavelengths generated by the time-evolution of control and carbonated specimens, using the ultrasonic pulse velocity of each transducer for a water/cement ratio of 0.50.

Frequency (kHz)	Diameter of Transducer (D) (mm)	Control wavelength (λ) (mm)		Carbonated wavelength (λ) (mm)	
		Mean ($M_{\lambda Co}$)	Std dev	Mean ($M_{\lambda Ca}$)	Std dev
Longitudinal wave transducer					
100	42	28.63	0.23	28.60	0.08
250	42	10.08	0.13	9.96	0.06
500	29	5.07	0.03	5.01	0.02
Transversal wave transducer					
100	29	24.16	0.24	24.16	0.13
250	29	10.00	0.16	9.88	0.06

4.2.3. Cement paste samples with water / cement ratio of 0.40

Figure 5 shows the results of the ultrasonic measurements for the control and carbonated specimens with w/c ratio = 0.4. As can be seen in Figure 5a- 5c, it was difficult to distinguish between control and carbonated specimens for this w/c ratio, neither using longitudinal wave transducers of frequencies of 100 and 250 kHz, nor 100 kHz transversal wave transducers. The behavior observed of the carbonation index was rather constant in comparison with the results of the previous w/c ratio analyzed. Even with the decrease of the wavelength, it cannot be assessed the carbonation degree of the specimens. The lower penetration in these specimens was caused

by the porosity reduction and the carbonation reaction on the surface of the specimens which prevent the penetration of CO_2 [19].

The correlation gets stronger between the FTIR data and the energy percentage calculated for the 250 kHz transversal wave transducer. The formation of solid calcium carbonated in the cement paste produced a higher interaction with the propagation of transversal waves, since they prefer to propagate through solid media [30]. This preference allows the wave for better detection of changes caused by the carbonation process in comparison with the longitudinal wave transducer of the same frequency (even with similar wavelengths, Table 3), enabling the distinction between the control and the carbonated cement paste even if the carbonation was at onset.

In Figure 5e, the results of the 500 kHz longitudinal wave transducer are shown. It was possible to distinguish the behavior between the control and the carbonated specimen, since the wavelength was the smallest produced (Table 3). The correlation with the FTIR data was stronger than with the others frequencies [13]. As stated, this was due to the size of the wavelength and also to the interaction of the longitudinal wave with the varying media. However, the standard error of the carbonation index increases with time because of the high sensitivity of the high frequency transducer.

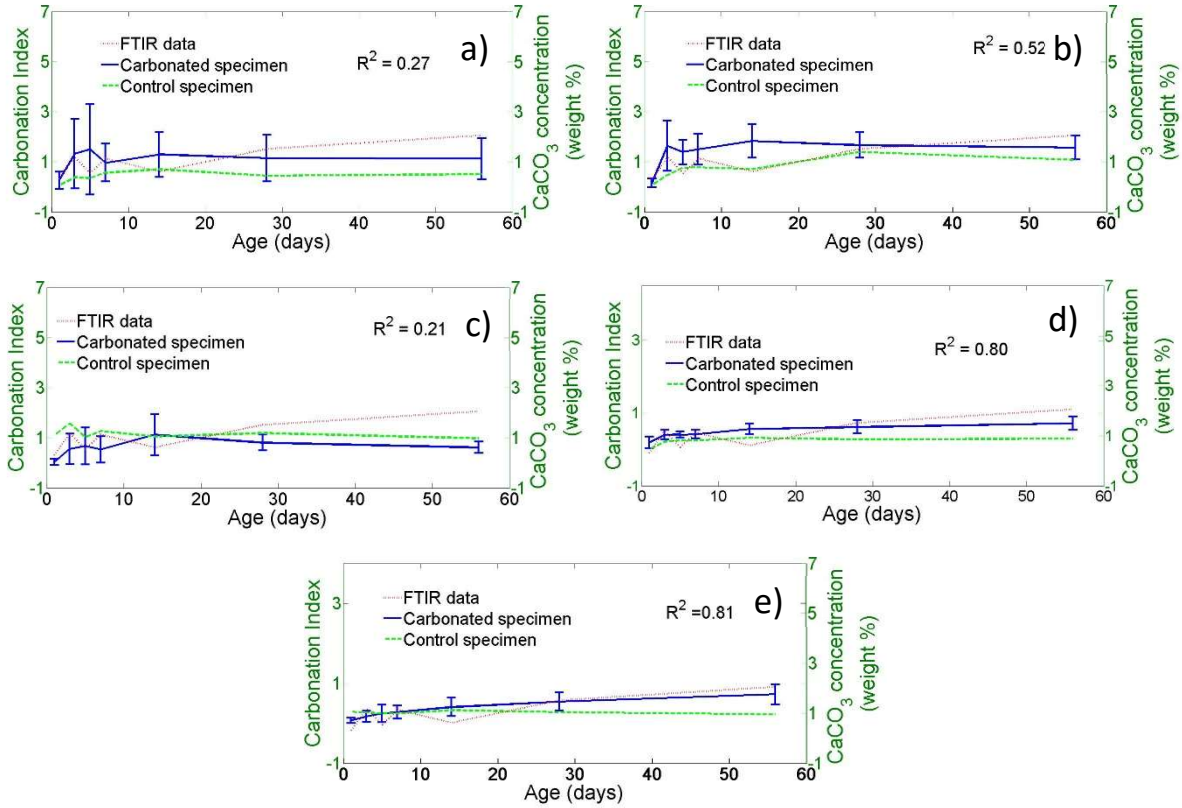

Figure 5. Evolution of carbonation index and content of calcium carbonate by FTIR, versus testing age for longitudinal wave transducer 100 kHz (a), 250 kHz (c), 500 kHz (e) and transversal transducer 100 kHz (b), 250 kHz (d) for cement paste specimens with w/c ratio = 0.40.

Variations in wavelength are shown in Table 3. Although, the wavelength of the control and carbonated specimens was very similar, the small changes in the wavelength are caused by the carbonation process. Also, the wavelength of the different wave type transducers and same frequency are very close one to another.

Table 3. Wavelengths generated by the time-evolution of control and carbonates specimens, using the ultrasonic pulse velocity of each transducer for a water/cement ratio of 0.40.

Frequency (kHz)	Diameter of Transducer (D) (mm)	Control wavelength (λ) (mm)		Carbonated wavelength (λ) (mm)	
		Mean ($M_{\lambda Co}$)	Std dev	Mean ($M_{\lambda Ca}$)	Std dev
Longitudinal wave transducer					
100	42	28.63	0.23	28.60	0.08
250	42	11.55	0.07	11.53	0.03
500	29	5.82	0.06	5.83	0.01
Transversal wave transducer					
100	29	27.67	0.20	27.97	0.28
250	29	11.43	0.10	11.50	0.04

As can be seen in Table 3, the wavelength between the w/c of 0.50 and 0.40 was almost the same, but in the w/c of 0.60, the wavelength was smaller. This was an indicator of the higher porosity of these specimens [24]. The close value of the control wavelength to the carbonated specimen wavelength, can explain the atypical results shown in Figure 3a, compared with the results shown in Figure 4a, where a clear differentiation between carbonated and control specimen can be observed. In the case of Figure 5a, the sensitivity was not enough to differentiate between the control and the carbonated specimen. However, unlike the Figure 3a, both behaviors remained constant, which was an indication that the carbonation front had not advanced enough to be detected and the response behavior seems to be constant, contrary with the results of Figure 3a, where the control specimen had an abnormal behavior.

In Figure 3b, the abnormal behavior of the control specimen was even more obvious since the index associated to it had significantly atypical, showing values below zero, which are inconsistent with the rest of the results. In Figure 4b the differentiation between control and carbonated specimen was better than in the rest of the measurements. The increase of the

wavelength, observed with the 100 kHz transversal wave transducers, is a parameter that indicates an increasing density of the specimens, with the reduction of the w/c ratio, better than the longitudinal wave transducer of the same frequency, as showed in Table 1-3.

Figure 3c, show an improvement in the distinction between the control and carbonated specimen almost as good as Figure 4c, where a clearer distinction between the carbonated and control specimen was possible, compere with Figure 5c. As the transducer frequency employed rise the distinction between the cement past was more clear, as the gap between wavelength increase, being the biggest one among the w/c ratio of 0.6 and 0.4.

As can be seen in Figure 4d and 5d, the evaluation of the carbonation improves, even for the w/c ratio of 0.40, which before were unresponsive, except for the w/c ratio of 0.60. Both cases are related to the decrease of the wavelength, as can be seen in Table 1-3, also the asses of the degree of carbonation had a strong correlation to the one obtained with the FTIR results.

In the case of the results show in Figure 4e and 5e, the carbonation index had the strongest correlation with the FTIR data of all measurements. This behavior was due to the small wavelength, as show in table 1-3, and the property of the longitudinal waves to travel true all media, which allows the ultrasound wave, to interact with a larger amount of material without losing energy, enabling a better assess of the carbonation degree, regardless of the w/c ratio.

5. Conclusions

The following conclusions are drawn based on the results obtained in this paper:

1. The non-destructive carbonation index based on ultrasound measurements, allows to determine the carbonation degree of the cement pastes studied (w/c = 0.60, 0.50 and 0.40), assuming that the carbonation products will progressively change the frequency spectra in time. The observed trends in the carbonation index are in agreement with the FTIR intensities observed for $CaCO_3$ generation.
2. For the cement pastes with w/c = 0.40, only the 250 kHz transversal wave transducer and the 500 kHz longitudinal wave transducer permit detection of the carbonation.
3. The carbonation index associated to w/c = 0.50 had a strong correlation with the FTIR results, especially with the 100 and 250 kHz longitudinal wave transducers.
4. The 250 kHz longitudinal wave transducers were able to distinguish between the carbonated and control specimens, as well as to assess the degree of carbonation in the w/c = 0.60, despite the atypical behavior of the control specimen.

References

[1]. L. Bertolini, B. Elsener, P. Pedeferri, E. Redaelli, R.B. Polder, Corrosion of Steel in Concrete: Prevention, Diagnosis, Repair, John Wiley & Sons, 2013

[2]. J.P. Broomfield, Corrosion of Steel in Concrete: Understanding, Investigation and Repair, CRC Press, 2002.

[3]. Neville, A. M., & Brooks, J. J. (1987). Concrete technology.

[4]. V. Papadakis, M. Fardis, C. Vayenas, Effect of composition, environmental factors and cement-lime mortar coating on concrete carbonation, Mater. Struct. 25 (5) (1992) 293–304.

[5]. N. Hyvert, A. Sellier, F. Duprat, P. Rougeau, P. Francisco, Dependency of C–S–H carbonation rate on CO_2 pressure to explain transition from accelerated tests to natural carbonation, Cem. Concr. Res. 40 (11) (2010) 1582–1589.

[6]. C.D. Atis, Accelerated carbonation and testing of concrete made with fly ash, Constr. Build. Mater. 17 (3) (2003) 147–152.

[7]. Papadakis, V. G., Vayenas, C. G., & Fardis, M. N. (1991). Physical and chemical characteristics affecting the durability of concrete. Materials Journal,88(2), 186-196.

[8]. P.H. Borges, J.O. Costa, N.B. Milestone, C.J. Lynsdale, R.E. Streatfield, Carbonation of CH and C–S–H in composite cement pastes containing high amounts of BFS, Cem. Concr. Res. 40 (2) (2010) 284–292.

[9]. S. Roy, K. Poh, D. Northwood, Durability of concrete—accelerated carbonation and weathering studies, Build. Environ. 34 (5) (1999) 597–606.

[10]. Chang, C. F., & Chen, J. W. (2006). The experimental investigation of concrete carbonation depth. Cement and Concrete Research, 36(9), 1760-1767.

[11]. T. Fukushima, Y. Yoshizaki, F. Tomosawa, K. Takahashi, Relationship between neutralization depth and concentration distribution of CaCO3–Ca(OH)2 in carbonated concrete, V.M. Malhotra (Ed.), Advances in Concrete Technology, ACI SP–179, Tokushima, Japan (1998), pp. 347–363.

[12]. V.G. Papadakis, M.N. Fardis, C.G. Vayenas, Hydration and carbonation of pozzolanic cements, ACI Mater. J., 89 (2) (1992), pp. 119–130.

[13]. X.F. Gao, Y. Lo, C.M. Tam, C.Y. Chung, Analysis of the infrared spectrum and microstructure of hardened cement paste, Cem. Concr. Res., 29 (1999), pp. 805–812.

[14]. Villain, G., & Thiery, M. (2006). Gammadensimetry: A method to determine drying and carbonation profiles in concrete. NDT & E International, 39(4), 328-337.

[15]. Chaix, J. F., Garnier, V., & Corneloup, G. (2003). Concrete damage evolution analysis by backscattered ultrasonic waves. NDT & E International, 36(7), 461-469.

[16]. Vincent Garnier, Bogdan Piwakowski, Odile Abraham, Géraldine Villain, Cédric Payan, Jean François Chaix, Acoustic techniques for concrete evaluation: Improvements, comparisons and consistency Construction and Building Materials, 43 (2013), pp. 598–613.

[17]. Cosmes-López, M. F., Castellanos, F., & Cano-Barrita, P. F. D. J. (2017). Ultrasound frequency analysis for identification of aggregates and cement paste in concrete. Ultrasonics, 73, 88-95.

[18]. ASTM C31 / C31M-15ae1, Standard Practice for Making and Curing Concrete Test Specimens in the Field, ASTM International, West Conshohocken, PA, 2015

[19]. Parrott, L. J., & Killoh, D. C. (1989). Carbonation in a 36 year old, in-situ concrete. Cement and Concrete Research, 19(4), 649-656.

[20]. Mehta, P. K. (1986). Concrete. Structure, properties and materials.

[21]. P. Duhamel, M. Vetterli, Fast fourier transforms: A tutorial review and a state of the art, Signal Processing 19 (1990), 259-299.

[22]. P. Anugonda, J. S. Wiehn, J. A. Turner, Diffusion of ultrasound in concrete, Ultrasonics 39 (2001), 429–435.

[23]. A. Villarreal, S. Solis-Najera, L. Medina-Gómez, Application of Waterman-Truell and the Dynamic Generalized Self-consistent Models on Concrete, Physics Procedia 70 (2015), 437 – 441.

[24]. Punurai, W., Jarzynski, J., Qu, J., Kurtis, K. E., & Jacobs, L. J. (2006). Characterization of entrained air voids in cement paste with scattered ultrasound. NDT & E International, 39(6), 514-524.

[25]. Punurai, W., Jarzynski, J., Qu, J., Kim, J. Y., Jacobs, L. J., & Kurtis, K. E. (2007). Characterization of multi-scale porosity in cement paste by advanced ultrasonic techniques. Cement and Concrete Research, 37(1), 38-46.

[26]. Qasrawi, H. Y. (2000). Concrete strength by combined nondestructive methods simply and reliably predicted. Cement and concrete research, 30(5), 739-746.

[27]. F. Aydin, M. Saribiyik, Correlation between Schmidt Hammer and destructive compressions testing for concretes in existing buildings, Sci. Res. Essays 5 (13) (2010) 1644–1648.

[28]. Cagnon, H., Vidal, T., Sellier, A., Soula, C., Bourbon, X., & Camps, G. (2016). Effects of water and temperature variations on deformation of limestone aggregates, cement paste, mortar and High Performance Concrete (HPC). Cement and Concrete Composites, 71, 131-143.

[29]. Chekroun, M., Le Marrec, L., Abraham, O., Durand, O., & Villain, G. (2009). Analysis of coherent surface wave dispersion and attenuation for non-destructive testing of concrete. Ultrasonics, 49(8), 743-751.

[30]. Métais, V., Chekroun, M., Le Marrec, L., Le Duff, A., Plantier, G., & Abraham, O. (2016). Influence of multiple scattering in heterogeneous concrete on results of the surface wave inverse problem. NDT & E International, 79, 53-62.

[31]. Chaix, J. F., Garnier, V., & Corneloup, G. (2006). Ultrasonic wave propagation in heterogeneous solid media: Theoretical analysis and experimental validation.Ultrasonics, 44(2), 200-210.

[32]. Akkaya, Y., Voigt, T., Subramaniam, K. V., & Shah, S. P. (2003). Nondestructive measurement of concrete strength gain by an ultrasonic wave reflection method. Materials and Structures, 36(8), 507-514.

[33]. Abo-Qudais, S. A. (2005). Effect of concrete mixing parameters on propagation of ultrasonic waves. Construction and building materials, 19(4), 257-263.

[34]. Thiery, M., Villain, G., Dangla, P., & Platret, G. (2007). Investigation of the carbonation front shape on cementitious materials: effects of the chemical kinetics. Cement and Concrete Research, 37(7), 1047-1058.

Capítulo III

Ultrasound determination of chloride presence in cement paste

Mario F. Cosmes-López[1], Francisco Castellanos[2*], Prisciliano F. de J. Cano-Barrita[2], Arturo E. Ramírez-Ortiz[1]

[1] *PhD student at Instituto Politecnico Nacional, CIIDIR Unidad Oaxaca, Hornos No. 1003, Santa Cruz Xoxocotlán, Oaxaca, Mexico, C.P. 71230.*

[2] *Researcher at Instituto Politecnico Nacional, CIIDIR Unidad Oaxaca, Hornos No. 1003, Santa Cruz Xoxocotlán, Oaxaca, Mexico, C.P. 71230.*

Phone: + 52 951 5170610, Emails: mcosmesl1200@alumno.ipn.mx, fcastellanos@ipn.mx, pcano@ipn.mx and arturo_iciv@hotmail.com

*Corresponding author

Abstract

Durability of concrete structures depends on ability of the cover concrete to resist penetration of harmful substances. Chloride ingress disrupts the passive film formed on the steel surface causing corrosion. Traditional techniques used to determine chloride penetration involve destructive sampling and chemical analysis. In order to improve some properties of concrete, Portland cement is partially substituted with mineral additions such as silica fume and fly ash. This study is focused on the ability of longitudinal and transversal ultrasound waves to detect the presence of chlorides in cement paste specimens containing mineral admixtures. Eighteen cylindrical specimens measuring 65 mm in diameter and 100 mm in height were cast with a w/c ratio of 0.55, with 100% of ordinary Portland cement, 20% and 40% substitution of cement by class F fly ash and 10% substitution by silica fume. The specimens were moist-cured in a saturated lime solution at 23 ± 2 °C for 120 days to reach a high degree of hydration. After oven-drying to constant mass, three samples of each group were vacuum saturated (4.08 bar) with NaCl solutions of 0%, 16.5 % (2.8 M), and 33 % (5.6 M). Ultrasonic measurements were undertaken at 0, 1, 3, 7 and 14 days using ultrasonic transducer with frequencies ranging from 50 kHz to 2250 kHz. Results show that it is possible to distinguish between the samples with and without chlorides regardless of the mineral addition and between the mineral additions depending on its binding capacity.

Keywords: Chloride binding, ultrasound, fly ash, silica fume

1. Introduction

Chloride penetration leads to corrosion of the reinforcing steel in concrete structures [1]. Chlorides may already be present in the materials employed for the elaboration of concrete but normally they ingress from external sources such as marine environments or deicing salts [2]. Cement hydration products react to some extent with chlorides to form Friedel's salt, leaving some free chloride ions that are responsible for the steel corrosion [3,4]. Therefore, the chloride binding capacity of cement paste is an important factor that influences the durability of concrete structures exposed to chloride-rich environments [5,6].

The use of mineral admixtures, such as fly ash and silica fume, increases the chloride binding capability of cement paste depending on the degree of substitution of Portland cement [7]. Chloride ion ingress into the cover concrete occurs mainly by diffusion due to a concentration gradient. The rate of diffusion is controlled by the chemical and physical characteristics of the pore structure [8]. Chloride ingress also depends on the surface concentration, as well as environmental factors such as temperature and relative humidity [9], producing a non-uniform distribution of chloride ions in concrete [10]. In the case of partially saturated cover concrete, water will be drawn into the pore structure driven by capillary forces [11].

Determination of chloride ion content in concrete is performed by different methods such as Accelerated Chloride Penetration [12], which is used to determine the apparent coefficient of chloride ion diffusion into concrete. A reliable chloride concentration profile for high quality concrete is difficult to obtain, as the penetration depth may be insufficient at 90 days [13].

The Electrical Indication of Concrete Ability to Resist Chloride Ion Penetration [14] is a rapid test to determine concrete relative resistance to penetration chloride ions. The electrical resistivity assesses chloride ingress considering that chloride presence increases the electrical conductivity of concrete. Since electrical current is used, it affects all ions in the pore solution, not just chloride ions. Also, the measurements are made before a steady migration is achieved and the high voltage increases the temperature that affects the results.

Another method is the Electrical Migration Technique [15] which accelerates the movement of chloride ions by the use of a low intensity electrical field. Despite of reducing the temperature related to the use of an electrical current, there is still a significant drawback due to the employment of an electrical migration test.

The Ion Selective Electrode Method [16] determines free chlorides with an embedded sensor that assesses changes in potential related to chemical activity. Unfortunately, the range of evaluation is too narrow to assure a reliable measurement. These non-destructive methods are very sensitive to the moisture content and require a calibration relationship to ensure repeatability [17].

Ultrasound techniques such as ultrasound pulse velocity have been employed to detect the presence of internal defects in concrete structures. Low ultrasound frequency (50 kHz) are used for characterization of large defects [18]. Higher frequencies (0.5-1 MHz) have been demonstrated to be more suitable for detection of smaller variations related to concrete degradation [19]. The ultrasound pulse velocity is capable of detecting microstructural changes. The presence of cracks or aggregates in concrete strongly influence the scattering when the wavelength is of the same order, diminishing the sensitivity to such defects/components [20].

In this study, a signal processing technique of longitudinal and transversal waves produced at different frequencies was used for detecting the presence of chlorides in cement pastes with and without mineral additions. In order to increase the surface exposed to chloride binding, specimens were oven-dried to evaporate the free water and replace it with NaCl solutions at different concentrations.

2. Experimental procedure

2.1. Materials

Mexican ordinary Portland cement class 30RS (ASTM C150 Type I) was used. Eighteen cylindrical specimens measuring 65 mm in diameter and 100 mm in height were cast with a w/c ratio of 0.55, with 100% of ordinary Portland cement (OPC), 20% and 40% substitution of cement by class F fly ash (20FA and 40FA, respectively) and 10% substitution by silica fume (10SF). The cylinders were filled in two layers, compacted by applying sixty strokes on the base of the mold on each layer. Then the specimens were placed in a device designed to rotate the samples at a speed of 7 rpm to avoid sedimentation. After 1 day, the specimens were stripped and moist-cured in a saturated lime solution at 23 ± 2 °C for 120 days to ensure complete hydration, according to the standard ASTM C31 [21].

In order to have similar initial conditions, all specimens were vacuum saturated with deionized water for at least one hour to ensure full saturation. Then the specimens were weighed and placed in an oven at 105 °C for two days, until constant mass is achieved. Once the specimens reached room temperature, three specimens of each group were vacuum saturated (4.08 bar) with NaCl

solutions of 16.5 % (2.8 M), 33 % (5.6 M) and one with only deionized water. All samples were covered with parafilm to prevent moisture loss.

2.2. Method

2.2.1. Ultrasonic measurements

To perform ultrasonic measurements, transducers were placed and centered on the circular faces. The pressure exerted on the transducers was controlled by a constant mass of 2.5 kg. The same position of the transducers was kept in through transmission measurements at different times. Ultrasonic measurements were made at 0, 1, 3, 7 and 14 days with transducer frequencies ranging from 50 kHz to 2250 kHz, for the three solutions used (NaCl 0% (deionized water), 16.5% NaCl and 33% NaCl).

2.2.2. Determination of chloride binding isotherms by the equilibrium method

This method assumes that once the equilibrium between the external solution and the pore solution of the sample is reached, the reduction in the concentration of the external solution is due to chlorides bound by cement hydration products. Therefore, by knowing the initial and final concentrations, the volume of the external solution and the dry mass of the sample, it is possible the calculation of the amount of bound chlorides according to [22]:

$$C_b = \frac{35.453\ (C_i - C_e)}{w_{11}(1-\xi_{11})} \quad (1)$$

where C_b is the amount of bound chlorides in mg $Cl/$ per sample, V is the volume of the external solution in mL, C_i is the external solution initial concentration of chlorides in mol / L, C_e

is the concentration of free chlorides in equilibrium with the external solution in mol / L, 35,453 is the molar mass of chloride ion, w_{11} is the mass in grams of the sample at a relative humidity (RH) of 11% and ξ_{11} is the evaporable water content to 11% RH. The chloride isotherms for each cementitious system are shown in Fig. 1.

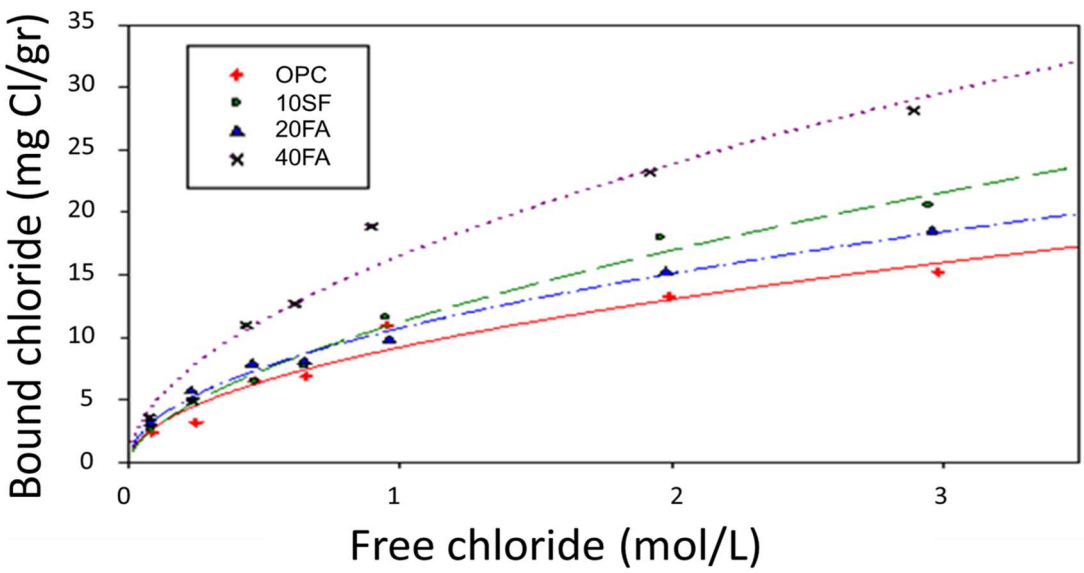

Fig. 1. Chloride binding isotherms for the four cementitious systems at a temperature of 23 °C for different chloride concentrations [23].

3. Wave analysis

3.1. Ultrasound signal processing

The herein proposed ultrasound signal processing to assess the presence of chlorides in the specimens was based on the method proposed in our previous work [24], to obtain a bound chloride index.

$$Ic=I-A \quad (2)$$

However, in order to distinguish between NaCl concentrations inside the different cement pastes, a standard deviation of the response of each concentration was obtained with respect to the response of water-saturated specimens.

4. Results and discussion

Fig. 2 shows the bound chloride index for the distinct cement pastes using the 50 kHz transverse wave transducers. Oven drying the samples caused extensive cracking that influenced the ultrasonic response of the cement pastes. This influence can be seen on the samples containing water. These specimens present changes that cannot be attributed to the hydration process as the samples were moist cured for an adequate period of time to ensure a high degree of hydration.

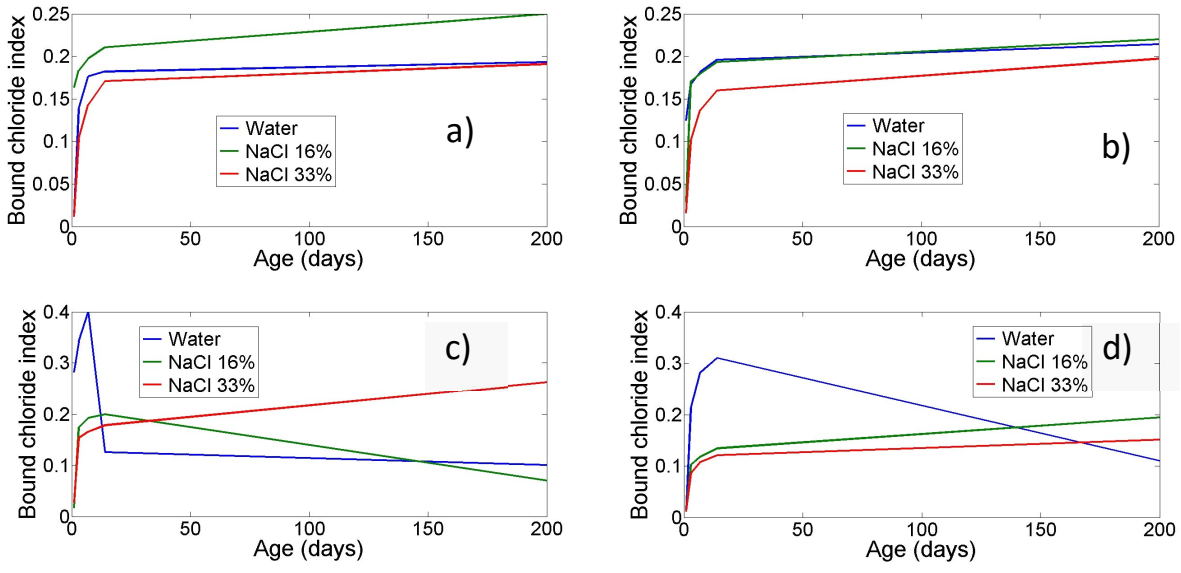

Fig. 2. Bound chloride Index obtained for all cement paste specimens containing a) 100 % Portland cement, b) 10% silica fume, c) 20 % fly ash, and d) 40 % fly ash. Transversal wave transducers of 50 kHz were employed.

These changes may be attributed to the movement of water inside the cement paste after vacuum saturation. It is possible that water did not completely filled all the gel pores. As a result, moisture redistribution by capillary forces may occur [25]. In addition, it is not expected that the penetration of water would significantly change the microstructure of the samples. On the other hand, chloride chemical binding will produce crystals of Friedel's salt that may affect the ultrasound response of the samples. It is possible to assess these changes by comparing the index obtained from the different chloride concentration specimens with the control specimen that contains only water.

The increase in concentration of the NaCl solutions inside the specimens will in turn increase the viscosity of the pore solution. Higher NaCl concentrations will also increase the amount of chemically and physically bound chlorides in the cement pastes [26, 27, 28, 29], provided the binding capacity is not exhausted. This will emphasize the different behavior among the specimens saturated with different concentrations (0%, 16% and 33% of NaCl). Changes in the microstructure of the different pastes are due to higher concentration of free chlorides in the pore solution that reacts with C3A [27]. The latter changes depicted, are reflected in the higher deviation from the specimens containing water.

As can be seen in Fig. 3, it is possible to distinguish the behavior between specimens containing NaCl solutions with different concentrations, aside of the transducer employed, due to the difference in average values of standard deviations.

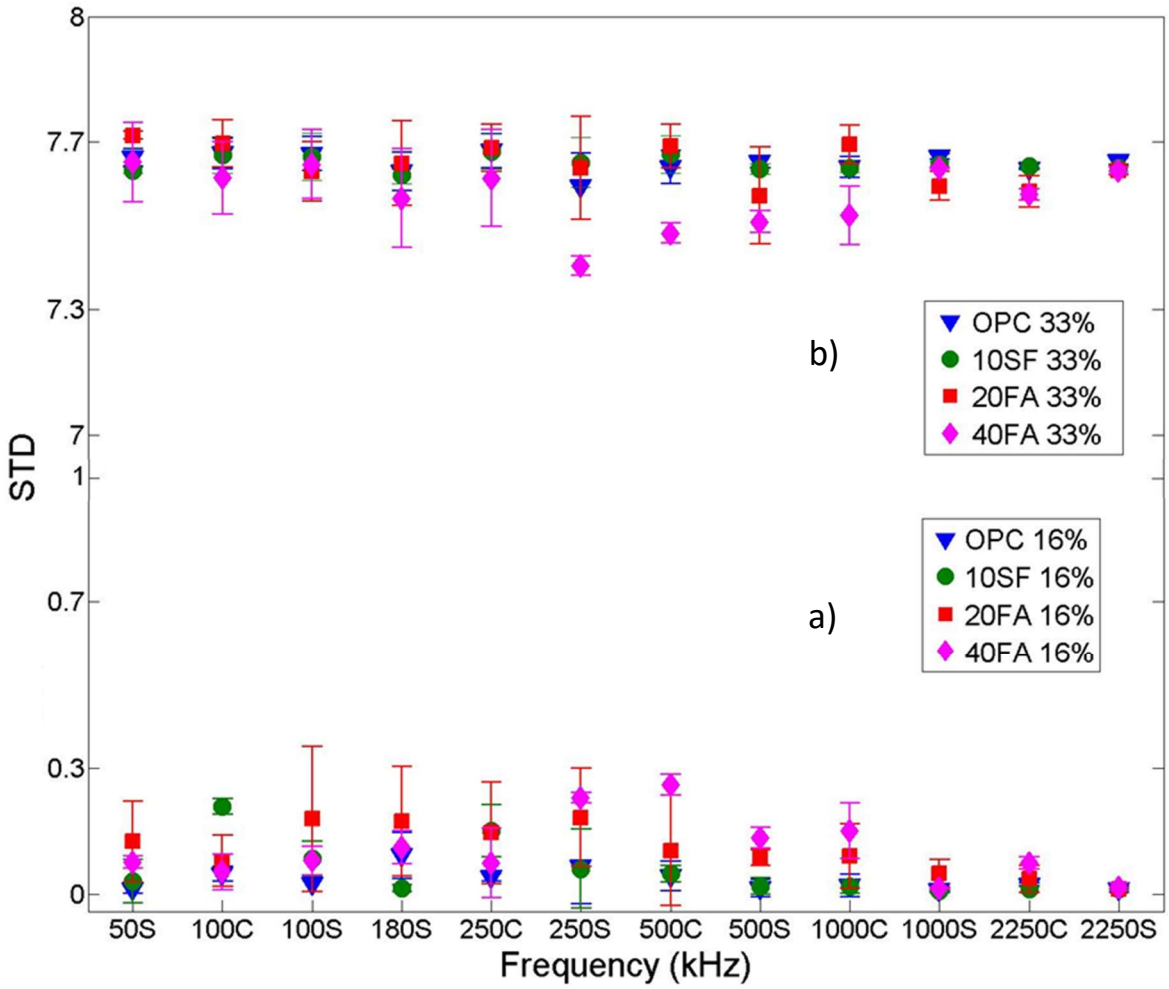

Fig. 3. Average values of the standard deviation obtained from a) 16 % NaCl solution, and b) 33 % NaCl solution, assuming as a mean of the process the response of the control specimens containing water, for all ultrasound transducers used.

Fig. 4 presents the standard deviation of the cement paste specimens with a 16% concentration of NaCl versus the control specimens containing water, for all ultrasound transducers. It is observed that the standard deviation is very low compared with the 33% concentration specimens. However, as shown in Fig. 4a, the low frequency transducers (50 to 180 kHz) are not sensitive to the microstructural changes, unlike the frequencies of 250 and 500 kHz, that are consistent with

the chloride binding isotherms shown in Fig. 1. This behavior may be associated with the higher sensitivity related to the higher frequencies employed, as well as by the preference of transversal waves to travel through the solid phase of the porous medium, modified by the formation of Friedel's salt [30].

In the case of Fig. 4b, transducers with frequencies from 500 to 2250 kHz show a similar behavior compared with the results of the chloride binding isotherms (Fig. 1). This behavior is not only due to wavelength but also because of the capability of the longitudinal waves to travel through fluid and solid media. Despite of this distinction, the reduction of the concentration of NaCl in the pore solution and the binding of the cement paste through the formation of Friedel's salt is more difficult to differentiate with this type of waves.

As can be seen, the longitudinal wave transducer from 500 kHz and above, had a better distinction between the four types of cement paste than the transversal wave transducer. At lower frequencies, the results are not consistent.

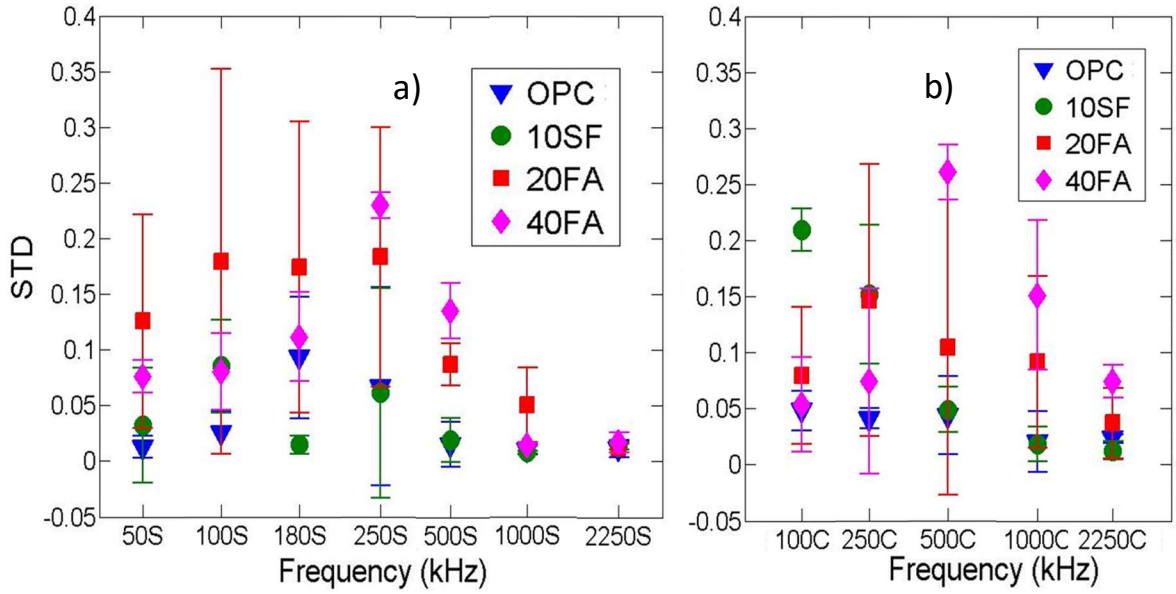

Fig. 4. Average values of standard deviation for 16 % NaCl solution of all cement paste samples using a) transversal wave transducers, and b) longitudinal wave transducers.

Fig. 5 shows results for the measurements on samples saturated with 33 % NaCl solution concentration. As can be seen, the standard deviation is higher than that of the 16 % NaCl concentration. In Fig. 5a the results of the transversal wave transducers show a lower dispersion of data, in comparison with the last concentration (Fig. 4a). The main feature is that the cement paste which has the highest binding capacity (40FA) produces a lower average value of the standard deviation than the other samples. These results may be attributed to the high chloride concentration, that caused an increase in the pore solution viscosity [31], decreasing the propagation through the pore structure. Another possible factor is the chemical chloride binding that obstructs the movement of the pore solution, and subsequently decreasing the ultrasound signal changes [32]. That may be the main reason why the most reactive cement paste is lower than the other cement pastes in all transducer frequencies (Fig. 5). However, the preference of the transversal wave to travel only through the solid phase impact on the high dispersion of the results. The results of the 250 kHz transversal wave transducer show an acceptable differentiation among the different cement pastes

Results of the longitudinal wave transducers are shown in Fig. 5b. As can be seen, the behavior is very similar to the transversal wave transducer. However, since the longitudinal waves are able to travel through fluid and solid media, the resulting data dispersion is lower than that of the transversal wave transducers. The higher frequencies ranging from 500 and 1000 kHz present a better differentiation among cement pastes. Unlike the results for 16% NaCl, in this case even for the lower frequencies it is possible to distinguish the different cement pastes

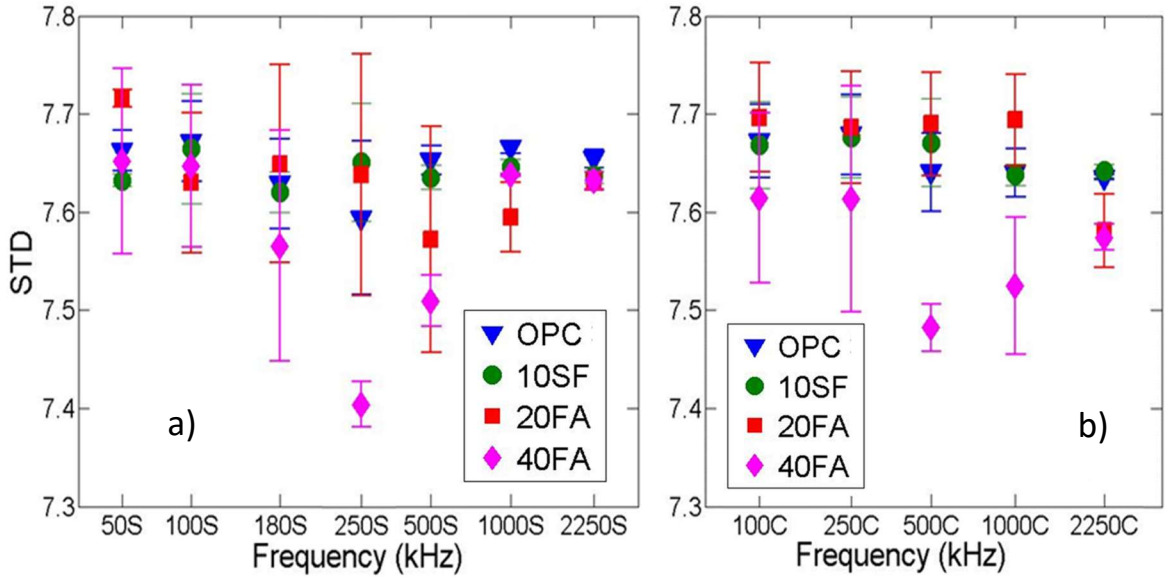

Fig. 5. Average values of standard deviation for 33% NaCl solutions for all cement paste specimens, a) transversal wave transducer, and b) longitudinal wave transducer.

5. Conclusions

1. It is possible to distinguish between the chloride concentrations of the solutions employed for saturating the samples (0 %, 16 % and 33 %) considering as reference the deionized water saturated specimens. This applies for all four-different cement pastes.
2. The results obtained with the proposed methodology, for the 16 % NaCl concentration it is consistent with the chloride binding isotherms, better identified with the 250 and 500 kHz transversal wave transducer and longitudinal wave transducer with frequencies of 500 kHz and higher, despite the extensive cracking of the specimens due to oven drying.
3. Results of the ultrasound signals analysis obtained with the methodology proposed, for the specimens saturated with 33 % NaCl concentration, are explained by the high concentration of chloride in the pore solution that increase the amount of chloride bound in the cement pastes, consuming the aluminates. This can be better appreciated in 250 kHz transversal wave transducer and for 500 and 1000 kHz longitudinal wave transducer.

References

[1]. Sánchez, I., Nóvoa, X. R., De Vera, G., & Climent, M. A. (2008). Microstructural modifications in Portland cement concrete due to forced ionic migration tests. Study by impedance spectroscopy. Cement and Concrete Research, 38(7), 1015-1025.

[2]. Neville Adam, Chloride attack of reinforced concrete: an overview, Materials and Structures (1995), Vol. 28, pp.63-70

[3]. G.K. Glass, N.M. Hassanein, N.R. Buenfeld, Magazine of Concrete Research 49 (1997) 323.

[4]. K. Byfors, Chloride initiated reinforcement corrosion, CBI Report 1:90, Swedish Cement and Concrete Research Institute, Stockholm, 1990, p. 5.

[5]. T. Luping, L.-O. Nillsson, Chloride binding capacity and binding isotherms of OPC pastes and mortars, Cem. Concr. Res. 23 (2) (1993) 247– 253.

[6]. P.S. Mangat, B.T. Molloy, Chloride binding in concrete containing PFA, gbs or silica fume under sea water exposure, Mag. Concr. Res. 47 (171) (1995) 129– 14

[7]. Mangat, P. S., & Molloy, B. T. (1995). Chloride binding in concrete containing PFA, GBS or silica fume under sea-water exposure. Magazine of concrete research, 47(171), 129-141.

[8]. Detwiler, R. J., Kjellsen, K. O., & Gjorv, O. E. (1991). Resistance to chloride intrusion of concrete cured at different temperatures. Materials Journal, 88(1), 19-24.

[9]. Bastidas-Arteaga, E., Chateauneuf, A., Sánchez-Silva, M., Bressolette, P., & Schoefs, F. (2010). Influence of weather and global warming in chloride ingress into concrete: A stochastic approach. Structural Safety, 32(4), 238-249.

[10]. Halamickova, P., Detwiler, R. J., Bentz, D. P., & Garboczi, E. J. (1995). Water permeability and chloride ion diffusion in Portland cement mortars: relationship to sand content and critical pore diameter. Cement and Concrete Research, 25(4), 790-802.

[11]. Delagrave, A., Marchand, J., & Samson, E. (1996). Prediction of diffusion coefficients in cement-based materials on the basis of migration experiments. Cement and Concrete Research, 26(12), 1831-1842.

[12]. Nordtest Method NT BUILD 443: Accelerated Chloride Penetration into Hardened Concrete, Nordtest, Espoo, Finland, Proj. 1154-94, 1995.

[13]. "Standard Method of Test for Resistance of Concrete to Chloride Ion Penetration", (T259-80), American Association of State Highway and Transportation Officials, Washington, D.C., U.S.A., 1980

[14]. Andrade, C. "Calculation of Chloride Diffusion Coefficients in Concrete From Ionic Migration Measurements" Cement and Concrete Research, Vol. 23, No, 3, pp. 724-742, 1993

[15]. Andrade, C. "Calculation of Chloride Diffusion Coefficients in Concrete From Ionic Migration Measurements" Cement and Concrete Research, Vol. 23, No, 3, pp. 724-742, 1993

[16]. Muralidharan, S., Vedalakshmi, R., Saraswathi, V., Joseph, J., & Palaniswamy, N. (2005). Studies on the aspects of chloride ion determination in different types of concrete under macro-cell corrosion conditions. Building and environment, 40(9), 1275-1281.

[17]. Basheer, P. A. M., Gilleece, P. R. V., Long, A. E., & Mc Carter, W. J. (2002). Monitoring electrical resistance of concretes containing alternative cementitious materials to assess their resistance to chloride penetration. Cement and Concrete Composites, 24(5), 437-449.

[18]. Basheer, P. A. M., Gilleece, P. R. V., Long, A. E., & Mc Carter, W. J. (2002). Monitoring electrical resistance of concretes containing alternative cementitious materials to assess their resistance to chloride penetration. Cement and Concrete Composites, 24(5), 437-449.

[19]. Naffa, S. O., Goueygou, M., Piwakowski, B., & Buyle-Bodin, F. (2002). Detection of chemical damage in concrete using ultrasound. Ultrasonics, 40(1), 247-251.

[20]. ChaixJF, GarnierV, CorneloupG. Ultrasonic wave propagation in hetero-geneous solid media: theoretical analysis and experimental validation. Ultrasonics 2006; 44:200–10.

[21]. ASTM C31 / C31M-15ae1, Standard Practice for Making and Curing Concrete Test Specimens in the Field, ASTM International, West Conshohocken, PA, 2015.

[22]. Luping, T., & Nilsson, L. O. (1993). Chloride binding capacity and binding isotherms of OPC pastes and mortars. Cement and concrete research, 23(2), 247-253.

[23]. Arturo Emanuel Ramírez Ortiz, Ultrasonido aplicado al estudio de la penetración y ligado de cloruros en pastas de cemento, Master thesis, Instituto Politécnico Nacional, 2012.

[24]. Cosmes-López, M. F., Castellanos, F., & Cano-Barrita, P. F. D. J. (2017). Ultrasound frequency analysis for identification of aggregates and cement paste in concrete. Ultrasonics, 73, 88-95.

[25]. Kanematsu, M., Maruyama, I., Noguchi, T., Iikura, H., & Tsuchiya, N. (2009). Quantification of water penetration into concrete through cracks by neutron radiography. Nuclear Instruments and Methods in Physics Research Section A: Accelerators, Spectrometers, Detectors and Associated Equipment, 605(1), 154-158.

[26]. Byfors, K., "Chloride Binding in Cement Paste", Nordic Concrete Research, Vol. 5, pp. 27-38, 1986

[27]. Rasheeduzzafar, Dakhil, F.D., Bader, M.A. and Khan, M.M., "Performance of Corrosion Resisting Steels in Chloride Bearing Concrete', ACI Materials Journal, Vol. 89, No. 5, pp. 439-448, 1992.

[28]. Kestin, J., Khalifa, H. E., Ro, S. T., & Wakeham, W. A. (1977). Preliminary data on the pressure effect on the viscosity of sodium chloride-water solutions in the range 10-40. degree. C. Journal of Chemical and Engineering Data, 22(2), 207-214.

[29]. Jacquemin, J., Husson, P., Padua, A. A., & Majer, V. (2006). Density and viscosity of several pure and water-saturated ionic liquids. Green Chemistry, 8(2), 172-180.

[30]. Suryavanshi, A. K., Scantlebury, J. D., & Lyon, S. B. (1996). Mechanism of Friedel's salt formation in cements rich in tri-calcium aluminate. Cement and concrete research, 26(5), 717-727.

[31]. Chenlo, F., Moreira, R., Pereira, G., & Ampudia, A. (2002). Viscosities of aqueous solutions of sucrose and sodium chloride of interest in osmotic dehydration processes. Journal of food Engineering, 54(4), 347-352.

[32]. Sawamura, S., Yoshimura, Y., Kitamura, K., & Taniguchi, Y. (1992). Effects of pressure, temperature, and concentration on the viscosity of an aqueous solution of sodium chloride. The Journal of Physical Chemistry, 96(13), 5526-5529.